SCALING AND EQUIVALENCY OF BENCH-SCALE TESTS TO FIELD SCALE CONDITIONS

Recycled Asphalt Pavement and Recycled Concrete Aggregate

TPF-5 (129) Recycled Unbound Materials

Mn/DOT Contract No. 89264 Work Order No. 2

CFMS Contract No. B14513

Task 1C: Scaling and Equivalency: Specimen Tests to Field-Scale Conditions

Gregory J. Schaertl, Tuncer B. Edil, and Craig H. Benson

University of Wisconsin- Madison

August 21, 2010

EXECUTIVE SUMMARY

The objectives of this study were to determine the resilient modulus for recycled materials using Large-Scale Model Experiments (LSME) to replicate field conditions. Tests were conducted on two recycled materials; recycled asphalt pavement (RAP) and recycled concrete aggregate (RCA), as well as on one blended material consisting of 50% RCA and 50% conventional base material (Class 5). The results of LSME testing were compared to the resilient modulus determined using laboratory methods in accordance with NCHRP 1-28a and field scale methods using falling weight deflectometer (FWD). The scalability of the laboratory results to field conditions was addressed by adjusting the resilient modulus to reflect a comparable stress-state and strain level. The plastic deformation of materials tested in the LSME was also assessed. A conventional base course meeting the gradation standard of a Minnesota Department of Transportation Class 5 aggregate was used as a reference material in this study.

The plastic deformation of RAP was 211% and 102% greater than that experienced by Class 5 for layer thicknesses of 0.3 m and 0.2 m, respectively, whereas the plastic deformation of RCA was 69% smaller than the plastic deformation experienced by the Class 5 for both layer thicknesses. The amount of deformation experienced by the blended RCA/Class 5 was 39% and 19% smaller for the 0.2-m and 0.3-m thick layers, respectively, indicating that the amount of deformation experienced in the base decreases with an increase in RCA. The amount of plastic deformation experienced by the RAP, RCA and Class 5 decreased with an increase in layer thickness. The plastic deformation of RAP and RCA

decreased 44% and 10%, respectively, for an increase in layer thickness from 0.2 m to 0.3 m. Class 5 experienced a reduction in plastic deformation of about 14% for an increase in layer thickness from 0.2 m to 0.3 m, which was slightly larger than the plastic deformation experienced by RCA, but significantly smaller than the plastic deformation experienced by RAP.

The summary resilient modulus (SRM) of RCA was 24% to 77% greater than that of Class 5, while the SRM of RAP was 18 to 33% greater. The SRM of the blended RCA/Class 5 was 17% to 29% greater than that of Class 5, which was comparable in magnitude to the SRM of RAP. The SRM of specimens increased with an increase in RCA content, although not in a linear manner. The cause of this non-linear behavior may be that the blended material is not a perfect 50%/50% blend. The SRM of all materials increased with an increase in layer thickness. The magnitude of this increase was common between the materials, and was between 130 MPa and 176 MPa.

The recycled granular material tested in the LSME is sensitive to layer thickness, indicating that the resilient modulus of the material is sensitive to varying strain levels. The resilient modulus was normalized to the low-strain (maximum) modulus, and plotted as a function of shear strain. The resulting plot suggests a backbone curve which describes the stress-strain dependency of resilient modulus for a given material. After applying corrections for stress-state and strain level, the resulting low-strain moduli for FWD, LSME and bench-scale tests were determined and found to be of the same magnitude within a reasonable amount of variance thus indicating the scalability of laboratory modulus to operating field modulus.

ACKNOWLEDGEMENTS

Thank you to my advisors, Professors Tuncer B. Edil and Craig H. Benson, for their guidance and support during my studies at the University of Wisconsin-Madison. Special thanks are extended to Professor James M. Tinjum for serving on my committee and to Professors Dante Fratta and James A. Schneider for providing scholarly insight. Much appreciation is extended to Ali Ebrahimi, Brian R. Kootstra, William G. Lang, and Xiaodong “Buff” Wang for helping to get the project started, and to Young-Hwan Son, Kyu Sun Kim, Timothy Alex Boecher, Logan Bailey, Jeff Casmer, Ozlem Bozyurt and Apisak Jutasiriwong for helping to keep the project going.

The past year and a half has been one of the most important and enriching periods of my life, and I owe it all to the friends and acquaintances I have made during that time. Their energy and support have kept me positive throughout my academic tenure, and will no doubt continue to inspire me as I embark on my professional career. This thesis is dedicated to all of them.

TABLE OF CONTENTS

LIST OF TABLES

LIST OF FIGURES

1. Introduction

The production of crushed stone aggregate in the United States was estimated at 2.2 billion metric tons in 1996, of which the U.S. highway system accounts for over 40 percent of the total demand (Grogan 1996). However, rapidly decreasing sources of virgin aggregate, along with limits placed upon aggregate production by environmental regulation and land use policies, has caused the price of these materials to increase dramatically (ACPA 2009). Conversely, the production of demolition and construction waste has increased as the amount of landfill available to contain this material has decreased (Poon et al. 2006, Chini et al. 2001). The need to find appropriate disposal locations for this material has been of increasing concern (Kuo et al. 2002). Recycling programs offer a viable solution to both problems.

The use of recycled materials as recycled base course in new or rehabilitated roadway construction has become more common in the last twenty years, with some municipalities reporting as much as 400,000 tons of recycled materials used in this manner (Bennert et al. 2000, Nataatmadja and Tan 2001). Recycled roadway materials are typically generated and used at the same construction site, providing increased savings in both money and time (Bennert et al. 2000). It has been speculated that in some municipalities recycled materials cost less to use than conventional crushed-stone base material by as much as 30% (Blankenagel and Guthrie 2006).

Recycled asphalt pavement (RAP) and recycled concrete aggregate (RCA) are materials commonly used as unbound base course in the construction of

roadway pavement. RAP is produced by removing and reprocessing existing asphalt pavement, and RCA is the product of the demolition of concrete structures such as buildings, roads and runways (Kuo et al. 2002, Guthrie et al. 2007, FHWA 2008). The production of RAP and RCA results in an aggregate that is well graded and of high quality, and the costs of recycled materials have been estimated to be 25% to 50% cheaper than traditional aggregates (Guthrie et al. 2007, FHWA 2008). Despite the increased acceptance of recycled base materials in construction, research concerning the mechanical properties and durability of such materials has been lacking (Bennert et al. 2000, Nataatmadja and Tan 2001, Guthrie et al. 2007).

The objectives of this study were to determine the resilient modulus and permanent deformations of RAP and RCA in the laboratory using Large-Scale Model Experiments (LSME) to simulate field conditions, and to determine the effect of varying RCA content and layer thickness on material stiffness. Scaling between LSME, typical bench-scale laboratory, and falling weight deflectometer (FWD) testing in a road section constructed of these materials is also discussed. This thesis describes the findings of the study.

2. Background

2.1. Production of Recycled Materials

Recycled asphalt pavement (RAP) and recycled concrete aggregate (RCA) are two materials commonly used as an alternative to virgin aggregate in roadway construction and rehabilitation. There is some ambiguity regarding the nomenclature involved in the production of RAP. RAP refers to the removal and reuse of the hot mix asphalt (HMA) layer of an existing roadway. Recycled pavement material (RPM) is a term used by some investigators to describe pavement materials reclaimed through a less precise process in which the HMA with either part of the base course layer or the entire base course layer with part of the underlying subgrade is reclaimed for use (Li et al. 2007, Wen and Edil 2009). Unless specified, these two distinct recycled asphalt materials will be collectively referred to as RAP.

RAP is typically produced through milling operations, which involve the grinding and collection of the existing HMA. RPM is typically excavated using full-size reclaimers or portable asphalt recycling machines (Guthrie et al. 2007, FWHA 2008). RAP can be stockpiled, but is most frequently processed immediately and reused on-site. Grading of RAP is typically achieved through pulverization with a rubber tired grinder (Bejarano et al. 2003). Typical RAP gradations resemble a crushed natural aggregate, with a higher content of fines resulting from degradation of the material during milling and crushing operations. The inclusion of subgrade materials in RPM can also contribute to higher fines content. Milling produces a finer gradation of RAP when compared to crushing (FHWA 2008).

RCA production involves crushing to achieve gradations comparable to typical roadway aggregate. Fresh RCA contains a high amount of debris and reinforcing steel that must be removed prior to placement. A jaw crusher breaks any debris from the RCA and provides an initial crushing. Debris is removed along a picking belt, and the remaining concrete is further crushed and screened to a specified gradation (Kuo et al. 2002). RCA is very angular in shape with a lower particle density and greater angularity than would normally be found in traditional virgin base course aggregates. Residual mortar and cement paste found on the surface of RCA contributes to a rougher surface texture, lower specific gravity, and higher water absorption compared to typical roadway aggregates (Kuo et al 2002, FHWA 2008).

2.2. Recycled Materials Used as Unbound Base Course

Several studies have been conducted comparing the mechanical properties of pure RAP and RCA with those of typical roadway base course aggregates. Bejarano et al. (2003) investigated the strength and stiffness of pure RAP compared to typical base course aggregate. Testing was performed on one RAP and two virgin base course aggregates. Individual specimens for each material were compacted at optimum moisture content (OMC) and at 95% and 100% of maximum wet density (MWD) according to CalTRANS specification CTM 216. Static triaxial tests were performed at confining pressures of 0, 35, 70 and 105 kPa. Stiffness tests were conducted according to AASHTO TP-46. Regardless of compaction effort, the shear strength of RAP and virgin aggregate were of comparable

magnitude, and the stiffness of RAP was greater than that of virgin aggregate. An increase in compaction effort increased the stiffness of RAP and one of the aggregate specimens, but had no effect on the second aggregate specimen.

Guthrie et al. (2007) evaluated the effects of RAP content on the shear strength and stiffness of roadway base course aggregate. Two RAP and two aggregates were chosen for the investigation. Specimens were prepared at RAP percentages of 100%, 75%, 50%, 25% and 0% (100% aggregate) for each of the possible RAP/aggregate permutations using modified compaction effort (ASTM D 1557). Specimen strength was determined by the California Bearing Ratio test (ASTM D 1883). Specimen stiffness was determined by free-free resonant column after compaction, after 72 hours of heating at 60°C to simulate summer conditions, and after an 11-day soaking/submerging period to simulate field saturation.

Specimen strength decreased with an increase in RAP content. The stiffness of specimens tested immediately after compaction decreased with the addition of 25% RAP, and then increased for RAP contents of 50%, 75%, and 100%. This trend reversed after 72 hours of heating: the stiffness of the material increased with the addition of 25% RAP, and then decreased for increased RAP content. Guthrie attributes this decrease in stiffness to the softening of asphalt during the heating process. After 11 days of soaking, the material maintained the same decrease-increase behavior as the heated specimen. However, the soaked materials displayed a 40% to 90% decrease in stiffness when compared to the heated material.

Kim et al. (2007) studied the effect of RAP content on the stiffness of blended aggregate base course. Stiffness tests were performed on pure RAP and aggregate samples and an in-situ blend of full-depth reclamation (FDR) material in accordance with National Highway Research Program testing protocol 1-28A (NCHRP 1-28a). Specimens were prepared at RAP percentages of 75%, 50%, 25% and 0% (i.e., 100% aggregate) and at moisture contents corresponding to 65% and 100% of OMC under standard compaction effort (AASHTO T 99). Stiffness increased for both an increase in RAP content and an increase in confining pressure. At higher confining pressures, the stiffness increased faster for specimens with higher RAP content. Specimens tested at 65% OMC had higher stiffness when compared to specimens prepared at 100% OMC at all confining pressures.

Bennert et al. (2000) investigated the shear strength of pure RAP and RCA compared to typical aggregate, and evaluated the effect of RAP and RCA content on the stiffness of blended aggregate base course. Strength tests were performed on one RAP, one RCA, and one aggregate sample. Specimens were compacted at maximum dry density (MDD) and OMC using standard compaction effort in accordance with methods described in AASHTO TP46-94, and loaded under drained static triaxial conditions at a common confining load of 103.42 kPa. Shear strength was higher for RCA than RAP; however shear strength was higher for pure aggregate than either RAP or RCA.

Stiffness tests were conducted according to AASHTO TP46-94. Specimens were prepared with RAP and RCA percentages of 100%, 75%, 50%, 25% and 0% (100% aggregate). Stiffness was higher for RAP and RCA than pure aggregate, and

increased with an increase in RAP or RCA content. RCA experienced lower permanent strain than pure aggregate; however RAP experienced higher permanent strain than RCA or pure aggregate. Bennert et al. (2000(suggest that the high permanent strains experienced by RAP may be due to either the breakdown of asphalt binder under loading or deficiencies inherent in the testing sequence itself.

Nataatmadja and Tan (2001) evaluated the relationship between the pre-crushing compressive strength and post-crushing stiffness of RCA. Four RCA with pre-crushing compressive strengths of 15, 18.5, 49 and 75 MPA were tested for stiffness according to methods proposed by Nataatmadja (1992). Each material was crushed and mixed to a particle size distribution comparable to typical roadway aggregate. Specimens were compacted at 89% of OMC using modified compaction effort (AS 1289.5.2.1). The stiffness of RCA increased with an increase in compressive strength from 15 MPa to 18.5 MPA, and again from 18.5 MPa to 49 MPa. However an increase in compressive strength from 49 MPa to 75 MPa resulted in a decrease in stiffness. Nataatmadja and Tan suggest that RCA with very high compressive strengths are more prone to break into elongated particles during crushing. Elongated particles were more prone to degradation after extensive loading, resulting in a lower stiffness than would otherwise be expected.

Camargo et al. (2009) compared the strength and stiffness of two recycled materials, RPM and recycled road surface gravel (RSG), to the strength and stiffness of an aggregate graded to the specifications for the Minnesota Department of Transportation (MnDOT) Class 5 base course. Specimen strength was determined by the California Bearing Ratio (CBR) test according to ASTM D 183,

and stiffness was determined by NCHRP 1-28a. The RPM and RSG each had a higher CBR than the typical base course aggregate, although all three materials had CBR values that were lower than the typically desired base course CBR value of 50. The RPM and RSG had a higher and lower stiffness, respectively, when compared to the Class 5 aggregate. The plastic strain experienced by the specimens during stiffness testing was lowest for RPM and highest for RSG and Class 5, which shared a plastic strain that was similar in magnitude.

Burrego et al. (2009) tested four RAP materials to quantify the variability of stockpiles in terms of gradation, asphalt content, and sand equivalency. An evident variation in gradation was noted for the RAP taken directly from stockpiles, although the variation was small after the material was subjected to ignition oven testing. The content of gravel, coarse sand, and fine sand were similar for each of the RAP samples. Burrego found that the asphalt content of RAP, which varied from 4.5% to 8.5%, had a significant effect on the gradation of the material. The sand equivalencies of the RAP samples were between 50 and 91.

2.3. Resilient Modulus

2.3.1. Definition of Resilient Modulus

Resilient modulus is a measure of a material's ability to deform elastically under cyclic compressive loading, and relates material stiffness to the mechanistic-empirical design method of pavements (NCHRP 1-37a). The performance of flexible pavement is dependent on the stiffness of the associated base course. Base course layers with higher resilient moduli are stiffer, incur less elastic deformation, and

transfer less stress to the overlying asphalt concrete and underlying subgrade. The reduction in fatigue cracking and rutting associated with this decrease in stress can have a positive effect on pavement life (Bejarano et al. 2003).

Resilient modulus testing involves cyclic loading of a specimen to simulate a moving wheel load. The elastic response of the specimen is recorded for various deviator and confining stresses. Elastic response is initially non-linear and the specimen experiences both plastic and elastic strains. When the applied deviator stress is small compared to the strength of the specimen, the plastic strain gradually dissipates and the remaining strain becomes almost entirely elastic and recoverable (Huang 2004). The linear-elastic modulus based on the recoverable strain is defined as resilient modulus, and is defined mathematically by Eqn. 2.1:

$$M_r = \frac{\sigma_d}{\varepsilon_r} \qquad (2.1)$$

in which ε_r is the recoverable elastic strain and σ_d is the applied deviator stress.

2.3.2. Factors that affect the Resilient Modulus of Unbound Aggregate

Several factors can influence the resilient behavior of a granular base course material, with stress-state having the greatest overall effect (Lekarp et al. 2000). Resilient modulus increases significantly with an increase in confining stress and decreases with an increase in deviator stress (Monismith et al. 1967, Hicks 1970). The effects of deviator stress are minimal to negligible for purely granular materials, depending on the amount of plastic deformation (Morgan 1966, Hicks and Monismith 1971). Moisture content can affect the stiffness of a granular material, but the extent to which this occurs depends on the degree of saturation. The stiffness of typical

granular specimens will stay nearly constant at lower saturation levels, but will decrease significantly as the saturation level rises (Hicks and Monismith 1971, Barksdale and Itani 1989). Lekarp et al. (2000) suggests that excess pore water pressures develop during cyclical loading for high degree of saturation, which decrease the strength and stiffness of the material.

Density, gradation and particle shape have been shown to have a small effect on the resilient modulus of granular material. Increased density contributes to an increased stiffness for granular material; however, increased fines content and increased crushing efforts appear to diminish these effects (Hicks and Monismith, 1971 Kolisojah 1997). Uniformly-graded specimens are stiffer than well-graded materials (Thom and Brown 1988); however the effects of moisture, fines content and particle angularity can increase the stiffness of well-graded aggregate to a degree equal-to or greater-than uniformly-graded aggregate (Plaistow 1994, Van Niekerk et al. 1998). Granular materials with angular to sub-angular particles have been found to have a higher resilient modulus than materials with rounded to sub-rounded particles (Hicks 1970, Thom and Brown 1989).

Research suggests that these influence factors also affect the resilient modulus of recycled aggregates. The resilient modulus of RAP and RCA has been shown to increase under the influence of increasing confining stress (Bennert et al. 2000, Molenaar and Van Niekerk 2002, Bejarano et al. 2003, Kim et al. 2007). Kim further found that increasing deviator stress decreased the resilient modulus of RAP, but had less of an effect than the confining stress. Tanyu et al. (2003) noted that

state of stress and strain amplitude had a significant effect on resilient moduli of various granular materials determined in both small and large-scale tests.

Kim et al. (2007) noted that RAP compacted at moisture contents less than optimum showed an increase in stiffness. Guthrie et al. (2007) found that RAP specimen stiffness decreased after extensive periods of saturation. Molenaar and Van Niekerk (2002) and Bejarano et al. (2003) found that increasing density increased the stiffness of RAP and RCA specimens, respectively. Molenaar and Van Niekerk (2002) also note that the gradation of RCA has limited influence on resilient modulus. Guthrie et al. (2007) found that the strength in RAP increased with particle angularity, although a correlation between angularity and stiffness could not be made.

2.3.3. Small-Scale Determination of Resilient Modulus of Unbound Aggregate

The linear-elastic response of unbound aggregate vary with different stress-states, with an increase in confining stress contributing to an increase in resilient modulus. Bench-scale laboratory tests subject a specimen to a sequence of deviator stresses and confining pressures and the resilient modulus of the specimen is determined by the elastic response. These sequences reflect typical field loading situations, and are defined by standards published by AASHTO or NCHRP guides.

One common power-function relating resilient modulus to bulk stress in granular materials is known as the K-θ model, and was proposed by Seed el al (1967), Brown and Pell (1967), and Hicks (1970). The K- θ model is presented in Eqn. 2.2:

$$M_r=k_1\left(\frac{\theta}{p_o}\right)^{k_2} \quad (2.2)$$

in which θ is the bulk stress, p_o is a reference stress (1 kPa), and k_1 and k_2 are empirically fitted constants for a given material. The bulk stress is expressed as the sum of the three principle stresses as defined in Eqn. 2.3:

$$\theta = \sigma_1 + \sigma_2 + \sigma_3 \quad (2.3)$$

The reference stress is an atmospheric constant used to eliminate the influence of pressure units on the calculated resilient modulus.

2.3.4. Large-Scale Model Experiments for Determination of Resilient Modulus of Unbound Aggregate

The Large-Scale Modeling Experiment (LSME) is a large prototype-scale test developed for simulating the performance of pavement sections in a laboratory setting. The advantage of the LSME testing is that it allows field conditions to be more accurately modeled than typical bench-scale testing methods. The pavement sections, or parts of them, are loaded cyclically to simulate field traffic loads and the resilient modulus is back calculated from the recorded response.

Falling weight deflectometer (FWD) is a non-destructive test used to determine the elastic modulus of pavement sections in the field. A weight of known mass is dropped from a designated height, and the deflection of the pavement at radial distances from the load location is recorded. The elastic modulus is back calculated from these measurements.

Tanyu et al. (2003) used LSME testing to determine the resilient modulus of typical base course material and two granular industrial by-products used as subbase materials. LSME test results were compared to resilient moduli determined from FWD and bench-scale tests. The summary resilient modulus is based on a bulk stress of 208 kPa as suggested for base course materials by NCHRP 1-28a sec 10.3.3.9, and calculated according to Eq. 2.2. The summary resilient modulus determined from the LSME and FWD tests were found to be similar in magnitude; however the summary resilient modulus determined from the bench-scale tests were found to be lower than those determined from LSME and FWD. Tanyu suggests that the LSME is a good indicator of the resilient modulus of field pavement sections, but that use of laboratory resilient modulus tests should be considered conservative at best. The resilient modulus measured in the LSME was also shown to be sensitive to thickness, with thicker layers having a higher stiffness. The modulus is dependent on strain amplitude: thicker layers contribute to wider stress distributions which lead to lower vertical strains (Seed 1970).

Kootstra et al. (2010) and Ebrahimi et al. (2010) used LSME testing to determine the deflection behavior and resilient modulus of a typical base course material and two recycled road materials, RPM and road surface gravel (RSG), used as base course material. The typical base course material was graded to MnDOT Class 5 aggregate specifications. Plastic strain and resilient modulus for each material were found to increase monotonically with the number of loading cycles. The plastic strain experienced by the Class 5 exhibited plastic shakedown, in which the plastic deformation ceased after an initial deformation period, and the plastic

strain experienced by the RPM and RSG experienced creep shakedown, in which the plastic deformation continued constantly during cyclic loading. Kootstra et al. (2010) suggest that the reason for the continuous plastic deformation was respectively due to the viscous deformation of the asphalt in RPM and the amount of plastic fines present in RSG. RPM and RSG were found to have a greater overall susceptibility to plastic deformation than Class 5. Summary resilient moduli determined by LSME testing was compared to bench-scale tests on the same materials conducted by Camargo et al. (2009); however, no clear correlation between the two methods could be made. Ebrahimi suggests that the difference between the summary resilient moduli determined by these two methods could be due to either a scale effect related to the volume of material involved, or to a difference in the strain amplitude experienced by each specimen.

Bejarano et al. (2003) used FWD testing to investigate the performance of RAP used in roadway rehabilitation. Tests were performed prior to rehabilitation on pavement consisting of asphalt concrete over typical unbound aggregate base course. The asphalt concrete was then pulverized and used as unbound base course for new roadway construction. Additional testing on the rehabilitated roadway indicated that the new pulverized RAP base course had a higher resilient modulus and resistance to shear strength compared to the original base course.

3. Materials and Methods

3.1. Materials

Two recycled materials, one conventional base material, and one blended recycled/conventional material were used in this investigation. The two recycled materials were a recycled asphalt pavement (RAP) and a recycled concrete aggregate (RCA), the conventional base material was a gravel meeting the MnDOT Class-5 specifications, and the blended material was a mix of approximately equal parts RCA and Class-5. The Class-5 material was used as the control material in this study. These materials are the same materials used in the roadway cells previously constructed at the MnROAD test facility in Maplewood, Minnesota and were obtained during construction. The Class-5 was salvaged from the base course of a previously constructed roadway cell. The RAP was milled from the surface of roadway cells also previously constructed at the MnROAD test facility. The RCA was obtained from a stockpile maintained by the Knife River Corporation at their pit located at 7979 State Highway 25 NE in Monticello, Minnesota. The blended material was mixed on site with the blade of a bulldozer prior to placement in the roadway cell.

A summary of the index properties, compaction test data and soil classifications for the four recycled materials is presented in Table 3.1. The RAP and Class-5 are classified as SP and A-1-b in the Unified Soil Classification System (USCS) (ASTM D 2487) and AASHTO Soil Classification System (AASHTO M 145), respectively. The blended RCA/Class 5 and RCA are classified as A-1-a according, and respectively as SP and GP according to USCS. Each of the materials used in

Table 3.1. Index properties for RAP, Class 5, RCA, and Blended RCA/Class 5.

Sample	D_{50} (mm)	C_u	C_c	w_{opt} (%)	$\gamma_{d\ max}$ (kN/m^3)	Asphalt Content (%)	LL (%)	PL (%)	Gravel Content (%)	Sand Content (%)	Fine Content (%)	USCS Symbol	AASHTO Symbol
RAP	1.51	6.9	0.7	6.7	20.8	4.8	NP	NP	26.3	71.2	2.5	SP	A-1-b
Class-5	1.63	9.9	0.6	8.0	20.7	-	NP	NP	32.8	65.4	1.8	SP	A-1-b
RCA	5.90	20.6	0.9	11.2	19.5	-	NP	NP	54.9	43.5	1.6	GP	A-1-a
Blend	3.35	18.8	0.4	8.9	20.1	-	NP	NP	44.6	53.4	2.0	SP	A-1-a

D_{50} = median particle size, C_u = coefficient of uniformity, C_c = coefficient of curvature, w_{opt} = optimum water content, $\gamma_{d\ max}$ = maximum dry density, LL = liquid limit, PL = plastic limit, NP = nonplastic.

Note: Particle size analysis conducted following ASTM D 422, $\gamma_{d\ max}$ and w_{opt} determined by ASTM D 1557 (AASHTO T-180), USCS classification determined by ASTM D 2487, AASHTO classification determined by AASHTO M 145 (ASTM D 3282), asphalt content determined by ASTM D 6307 (AASHTO TP-53), and Atterberg limits determined by AASHTO T-89 and T-90 (ASTM D 4318).

this study are classified as non-plastic. The particle size distribution curves for the four investigated materials as determined according to ASTM D 422 are shown in Fig. 3.1, along with the MnDOT specification for Class-5 used as a base course. Compaction tests were performed on each material using the modified compaction effort according to ASTM D 1557. Optimum water contents and maximum dry unit weights are summarized in Table 3.1, with associated compaction curves presented in Fig 3.2.

3.2. Small Specimen-Scale Testing

Small laboratory bench-scale resilient modulus tests were performed on compacted specimens according to NCHRP test protocol 1-28a (NCHRP 1-28a). Cylindrical specimens measuring 152 millimeters in diameter by 305 millimeters in length were prepared from each material. Specimens were prepared at optimum moisture content and compacted to 95% maximum dry density under modified compaction effort. Compaction of specimens was performed in six lifts of equal mass and stiffness to ensure uniform compaction.

Resilient modulus testing was carried out according to NCHRP 1-28a Procedure 1a, which applies to base and subbase materials. Deflections were measured via LVDTs positioned both internally and externally, with each LVDT having an accuracy of $\pm$0.005 mm. The specimens were loaded with an MTS Systems Model 244.12 servo-hydraulic machine. Loading sequences, confining pressures and data acquisition were controlled from a computer running LabView 8.5 software.

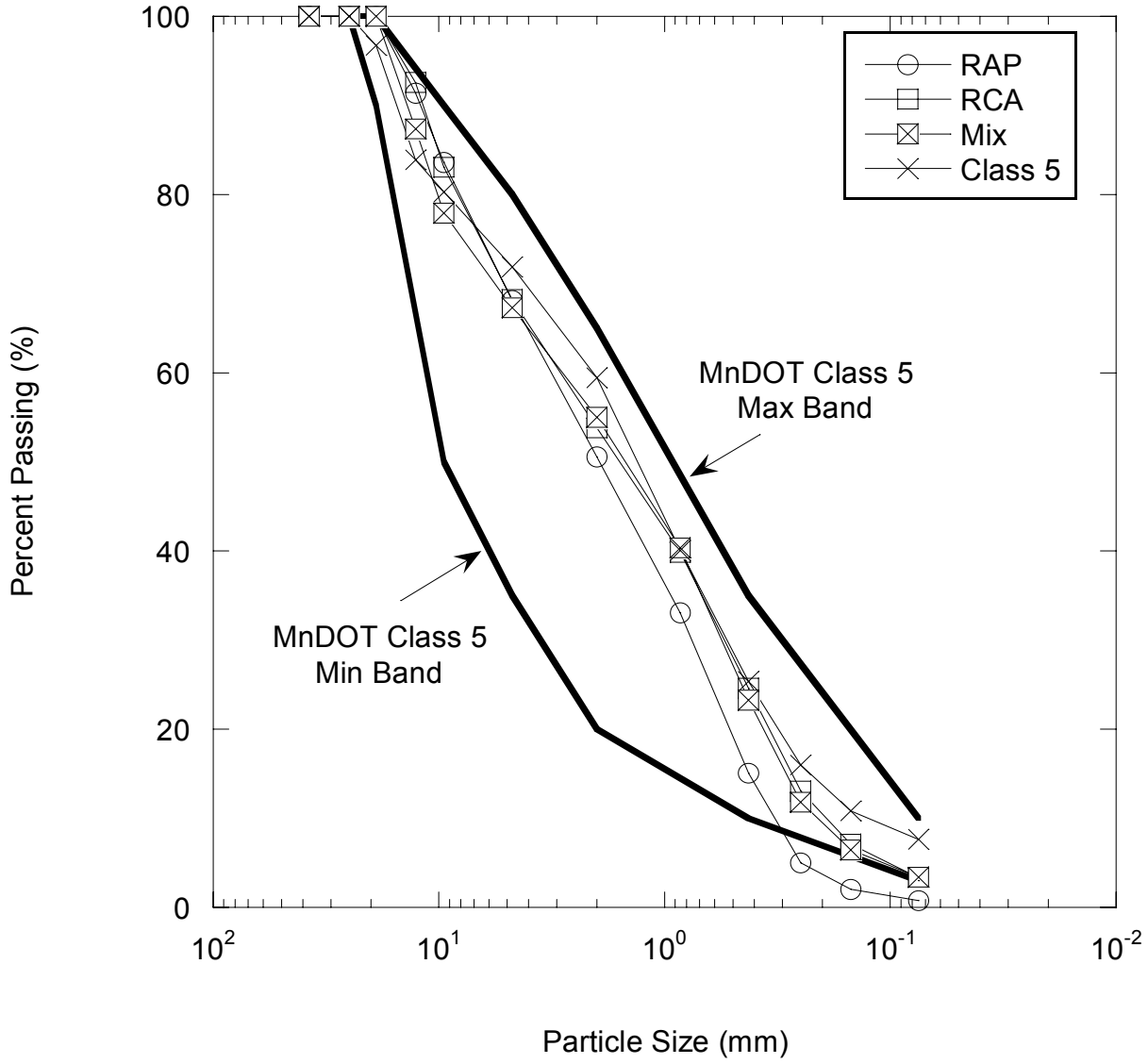

Fig. 3.1. Particle size distributions for RAP, RCA, Blended RCA/Class 5 and Class 5 with MnDOT specifications.

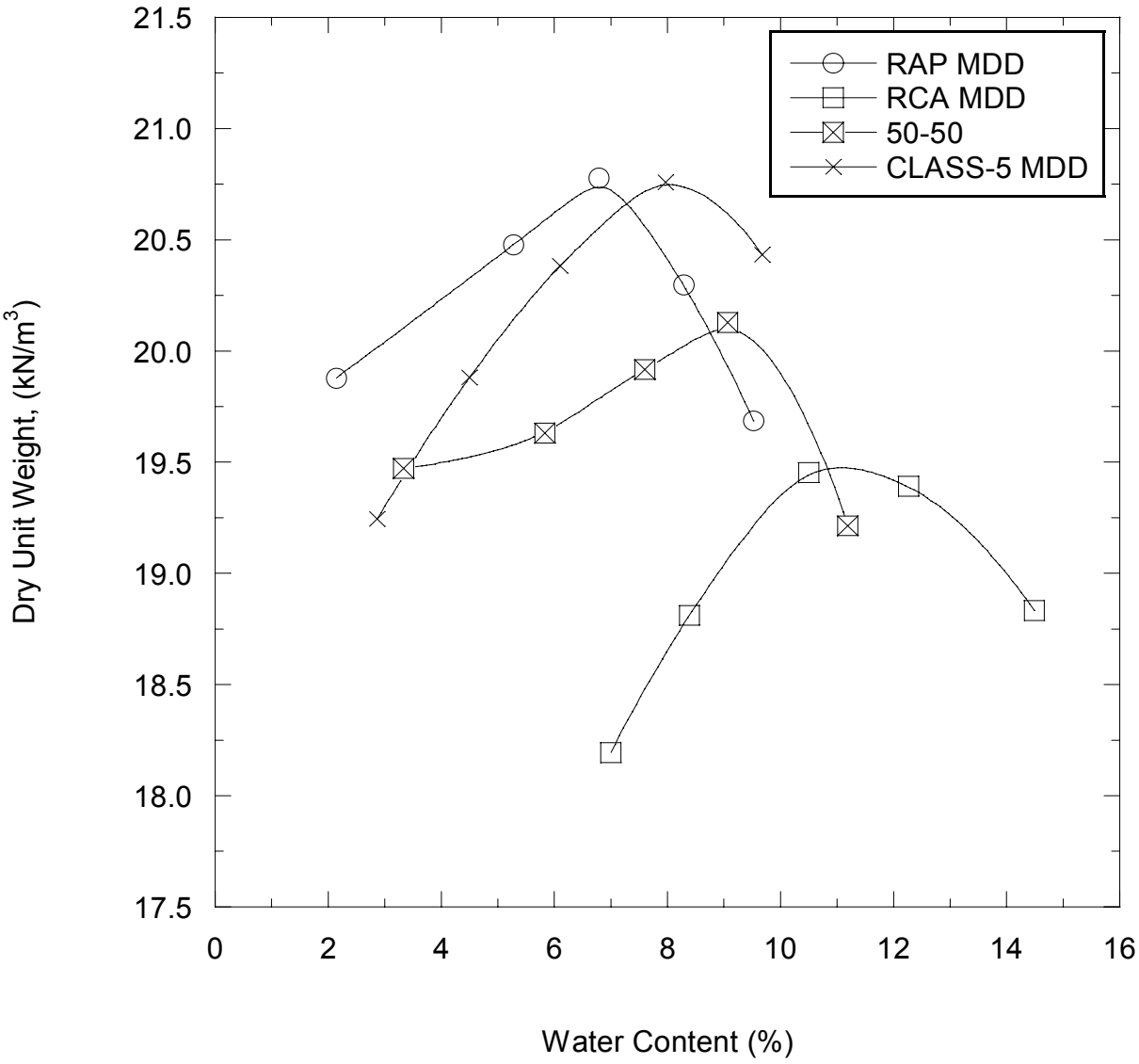

Fig. 3.2. Modified compaction curves for RAP, RCA, Blended RCA/Class 5 base, and Class 5.

The resilient modulus for each load sequence was obtained by averaging the resilient modulus from the last 5 cycles of each test sequence. The resilient modulus data were fit to the power function described by Eqn. 2.2. A summary resilient modulus was computed for each test at a bulk stress of 208 kPa, as suggested by Section 10.3.3.9 of NCHRP 1-28a. Further details of the specimen-scale laboratory testing methods are described by Son (2010) who performed the tests for unstabilized recycled materials.

3.3. Large-Scale Model Experiment

3.3.1. Apparatus and Loading Methodology

LSME is a modeling method used to determine the deflection of a pavement structure at prototype scale in a manner that replicates field conditions as closely as practical (Tanyu et al. 2003). A schematic of the LSME is shown in Fig. 3.3. Pavement profiles are constructed in a test pit with dimensions 3 m x 3 m x 3 m, and are subjected to 10,000 cycles of simulated traffic loading. The simulated loading is representative of a 4-axle truck applying a tire pressure of 700 kPa to a contact area of 0.05 m^2. Loads are generated by a MTS 280-L/m hydraulic actuator with a 100 kN force rating and 168 mm of stroke. Loads are applied to the pavement surface using a 25 mm thick circular steel plate with a radius of 125 mm. The pulse of the loading varies as a haversine function consisting of a 0.1 second load period followed by a 0.9 second rest period (Benson et al. 2009, Ebrahimi et al. 2010, Kootstra et al. 2010).

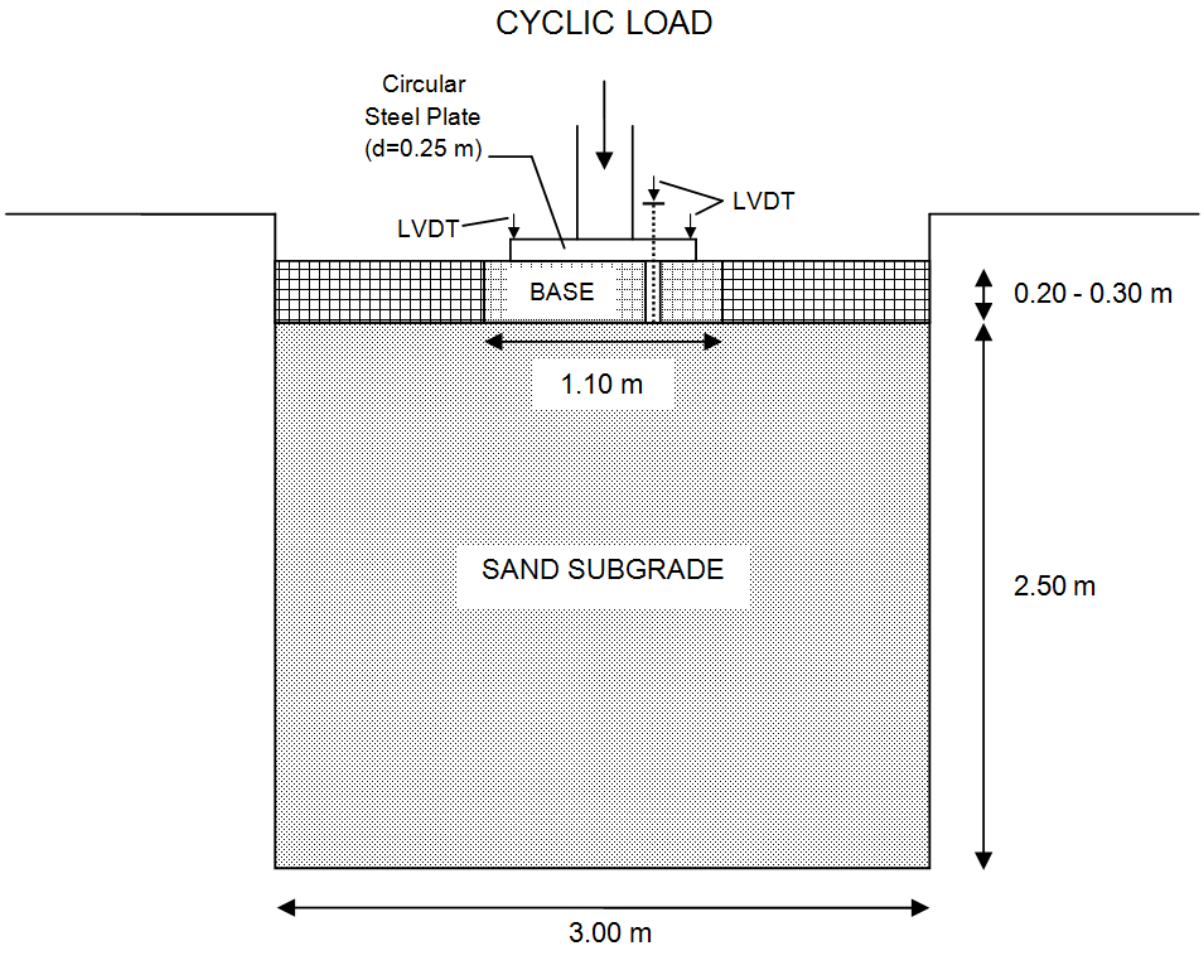

Fig. 3.3. Schematic of LSME testing setup.

The equivalent stress to be applied to the surface of the base course material in the absence of an asphalt layer was determined by non-linear finite-element analysis using the MICHPAVE program to model the performance of the proposed pavement profile (Benson et al. 2009, Kootstra et al. 2009). The base course was assumed to behave as non-linear elastic, and the asphalt surface and subgrade were assumed to behave as linear elastic. Loading and material properties used as inputs into the MICHPAVE program (Harichandran 1989) were determined from typical values (Huang 2004), and are presented in Table 3.2. The vertical stress distribution predicted by MICHPAVE is shown in Fig. 3.4. The vertical stress on the surface of the base layer is maximized directly below the center of loading, and decreases with an increase in radial distance. Based on a maximum stress of 133 kPa, a force of 6.7 kN was applied to base layer in the LSME with the loading plate. Previous LSME testing used the entire 3.0 m x 3.0 m test area to evaluate pavement performance (Tanyu et al. 2003, Benson et al. 2009, Kootstra et al. 2010). However, limited amounts of available base course materials made it necessary to reduce the evaluated test area to 1.0 m x 1.0 m. The remainder of the 3.0 m x 3.0 m test area was made up of recycled pavement material (RPM) to maintain the boundary stress that would otherwise be lost by a reduction in test area. The equivalency of this abbreviated test area and method of preparation are described in Appendix A. Pavement profiles consisted of 0.2 m to 0.3 m-thick of base course material over 2.5 m of dense, uniform sand subgrade. The performance of an asphalt layer was not central to the research, and therefore was not included in the LSME analysis.

Table 3.2. Inputs used for MICHPAVE for determining stress on base layer. (Adapted from Kootstra 2009)

Material Property of Load Condition	**Asphalt**	**Base**	**Subgrade**
Applied Load (kN)	35.0	6.7	NA*
Loading Radius (cm)	12.7	12.7	NA*
Thickness (cm)	12.7	20.3	NA*
Modulus (kPa)	3,300,000	398,000	48,000
k_1, k_2 (Eqn. 2.2)	NA*	27,600 kPa 0.5	NA*
Poisson's Ratio	0.35	0.35	0.45
Unit Weight (kN/m^3)	22.8	20.4	18.8

*NA = non-applicable

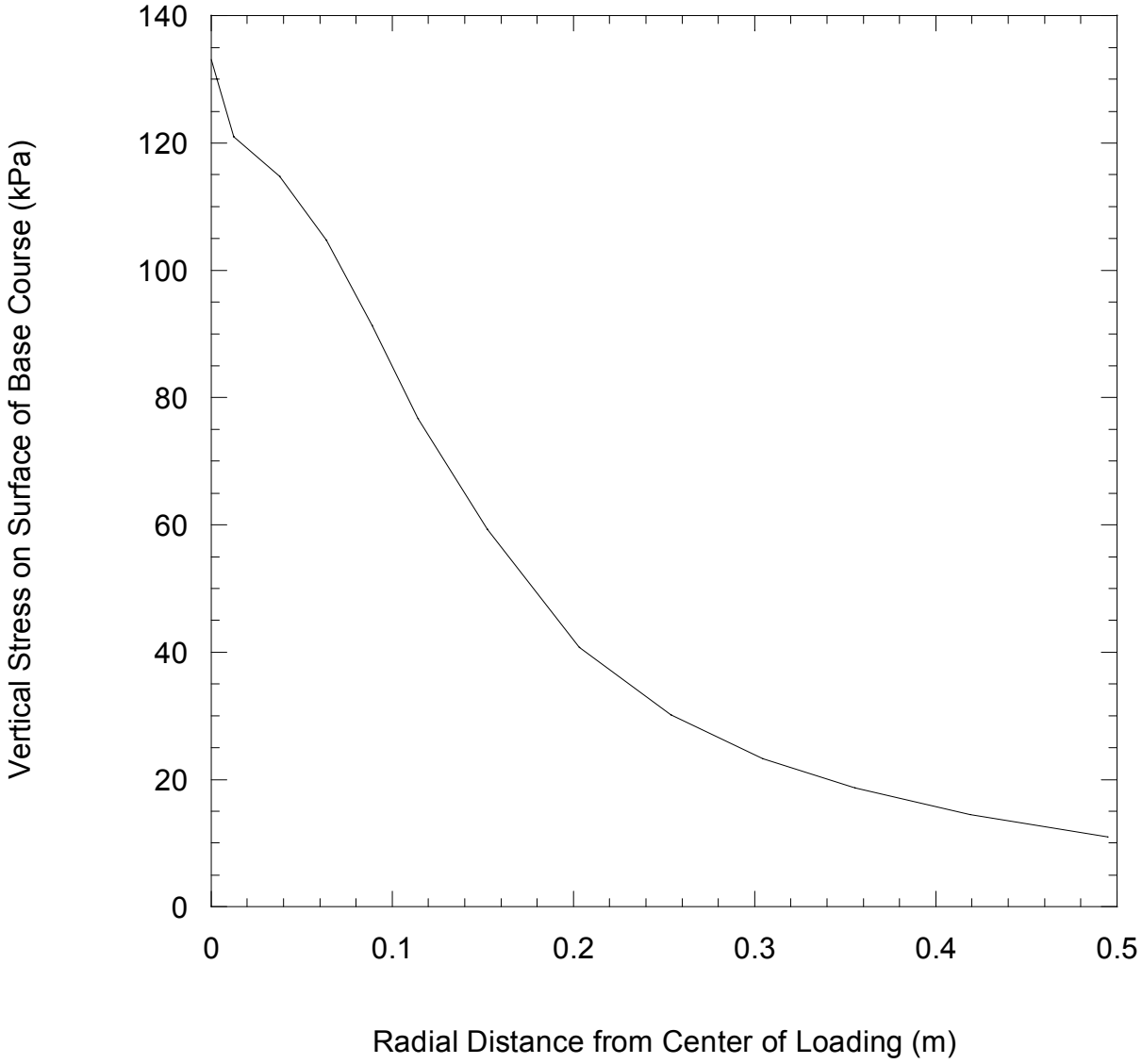

Fig. 3.4. Vertical stress on surface of base course vs. radial distance from center of traffic loading predicted by MICHPAVE.

3.3.2. Deflection Measurements

Vertical deflections at the surface of the base course and subgrade were measured during each loading cycle. Linear variable differential transducers (LVDT) were used to measure the deflections to a precision of $\pm$0.005 mm. Deflection of the base course was measured from the top of the loading plate, which was assumed rigid and able to translate the base course deflection. Subgrade deflections were measured by attaching small plates to either end of a thin rod extending through a tube extending through the loading plate and base course. One plate was laid flush with the subgrade surface while the other plate supported the LVDT located above the base course. Deflection of the subgrade was translated by the thin rod and measured by the LVDT. Deflections measured by the LVDTs were recorded using LabView 8.5 software.

3.3.3. Data Inversion

The resilient modulus of the base courses tested in the LSME was determined by performing a data inversion approach using MICHPAVE (Harichandran 1989). The elastic deflection of the base course was determined by subtracting the elastic deflection of the subgrade from the total elastic deflection of the profile as measured at the top of the base course. The LSME pavement profile was modeled as a two layer system in MICHPAVE. The elastic behavior of the base course and subgrade layers were modeled as non-linear and linear, respectively. The base course k_2 was determined from small-scale laboratory experiments in accordance with NCHRP 1-28a. The base course k_1 and subgrade elastic modulus

were varied until the elastic deflections predicted by MICHPAVE were within ±0.005 of those measured in the LSME. This method assumes that k_2 varies within a narrow range for a given material (Huang 2004) and follows the methods described by Tanyu et al. (2003) and Kootstra et al. (2009).

3.3.4. Base Course Compaction

Base course was compacted in lifts of approximately 0.10 m to efficiently and evenly distribute the modified compaction effort. Base course materials were prepared at optimum moisture content, and compacted to 95% of the modified maximum dry unit weight using a jumping-jack style compactor. A nuclear density gauge was employed to measure the in-situ dry unit weight and moisture content of each lift.

3.3.5. Field-Scale Falling Weight Deflectometer Testing

Field-scale in situ modulus of the materials was obtained from the Falling Weight Deflectometer (FWD) tests that were performed at the MnROAD testing facility in the roadway cells with the same materials tested in the small laboratory specimen tests and the LSME. Testing was performed using a trailer-mounted Dynatest model 1000 FWD. The FWD was controlled by an on-site computer which also recorded and stored load and deflection data. Three loads of 26.7, 40.0 and 53.4 kN were applied by the FWD to a 300-mm-diameter plate in contact with the pavement surface. Surface deflections were measured by nine load transducers

located at distances of 0, 0.30, 0.61, 0.91, 1.22, 1.52, and 1.83 meters from the center of the load.

The measured deflections were used to back-calculate the elastic modulus of the pavement layers using the MODULUS program developed at the Texas Transportation Institute. MODULUS uses linear-elastic theory to back-calculate elastic moduli from FWD data. The back-calculation was based on a three-layer model consisting of asphalt concrete, base course, and subgrade layers. Pavement profile and deflection data were provided by the MnDOT. The pavement profiles for the four test cells are presented in Fig. 3.5 The asphalt surface and base course layers were assigned a Poisson's ratio of 0.35, and the subgrade layer was assigned a Poisson's ratio of 0.40 (Huang 2004). The depth to the rigid layer was assumed to be at least 6 m and have little effect on the elastic moduli (Bush and Alexander 1985). The range of bulk stresses and vertical strains in the field was estimated using MICHPAVE. Surface loads taken from the FWD data and moduli from the MODULUS back-calculation were used as inputs. Structural layer coefficients were determined from the back-calculated moduli for use in pavement thickness design, as presented in Appendix B.

Cell 16: Recycled Concrete Aggregate (RCA)	Cell 17: Blended 50% / 50% RCA/Class 5 (Blend)	Cell 18: Recycled Asphalt Pavement (RAP)	Cell 19: Mn/DOT Class 5 Aggregate (Class 5)
127 mm Asphalt Concrete	127 mm Asphalt Concrete	127 mm Asphalt Concrete	127 mm Asphalt Concrete
305 mm RCA	305 mm Blend	305 mm RAP	305 mm Class 5
305 mm Class 3 Aggregate	305 mm Class 3 Aggregate	305 mm Class 3 Aggregate	305 mm Class 3 Aggregate
178 mm Select Granular Material	178 mm Select Granular Material	178 mm Select Granular Material	178 mm Select Granular Material
Clay	Clay	Clay	Clay

Fig. 3.5. Pavement profiles of cells tested using FWD at MnROAD testing facility. (Adapted from Johnson et al. 2009)

4. Results

4.1. Deflections in LSME

The total and plastic deflections at the surface of the base course and subgrade in the LSME as a function of loading cycle for RAP, RCA, blended RCA/Class 5, and Class 5 are presented in Figs. 4.1 thru 4.4. Deflections measured on the surface of the base course with thicknesses of 0.2 m and 0.3 m and subgrade are based on the haversine loading pulse. The total deflection is the peak deflection experienced during the 0.1-sec loading pulse, and the plastic deformation of each layer is the unrecovered deflection remaining during the 0.9-sec “at-rest” period. The amount of plastic deformation increases monotonically as the test progresses, with the greatest accumulation occurring during the first 50 loading cycles in all cases. The elastic deflection is the difference between the total and plastic deflections for each loading cycle. The net deflection represents the elastic deflection of the given base course layer and is the difference between the total elastic deflection measured at the surface and the elastic deflection of the subgrade. The elastic deflections at the surface and subgrade are presented as a function of loading cycle in Figs. 4.5 thru 4.8.

The net base elastic deflection for each of the materials slightly decreases as the cyclic loading progresses, which is caused by the gradual compaction of the particles into a denser matrix. The magnitude of the net elastic deflection for RAP and RCA were approximately equal for both layer thicknesses. The magnitude of the net elastic deflection for blended RCA/Class 5 and Class 5 is higher for the 0.2 m layer thickness than for the 0.3 m layer thickness. The thicker layer distributes the

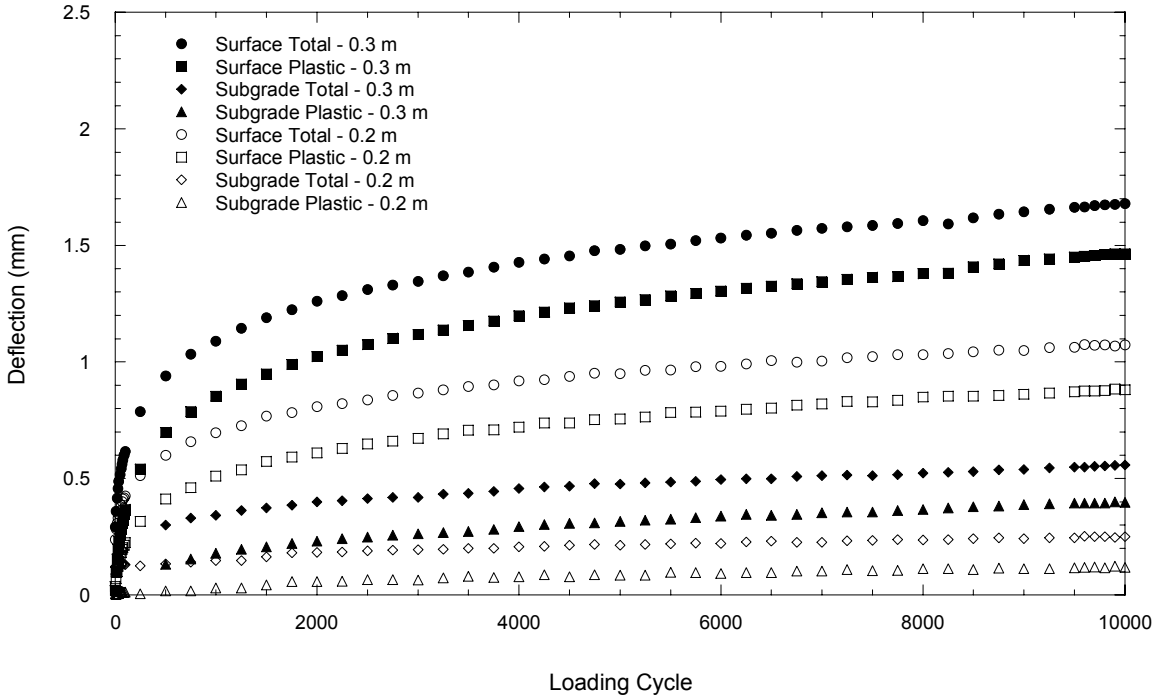

Fig. 4.1. Total and plastic deflection of surface and subgrade layers vs. number of loading cycles for RAP.

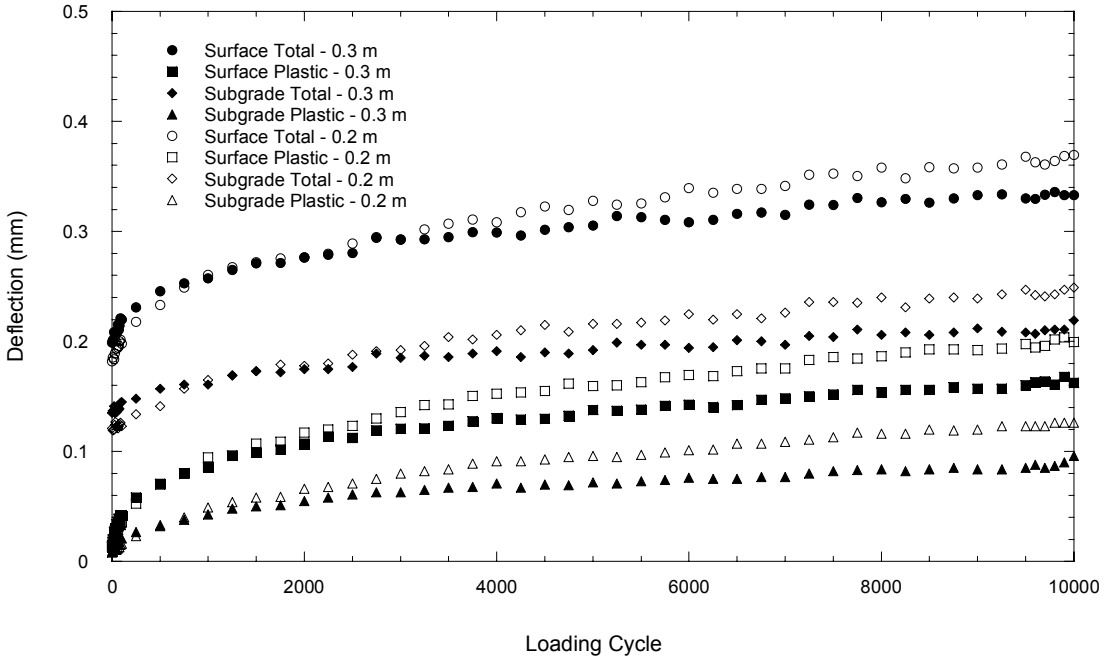

Fig. 4.2. Total and plastic deflection of surface and subgrade layers vs. number of loading cycles for RCA.

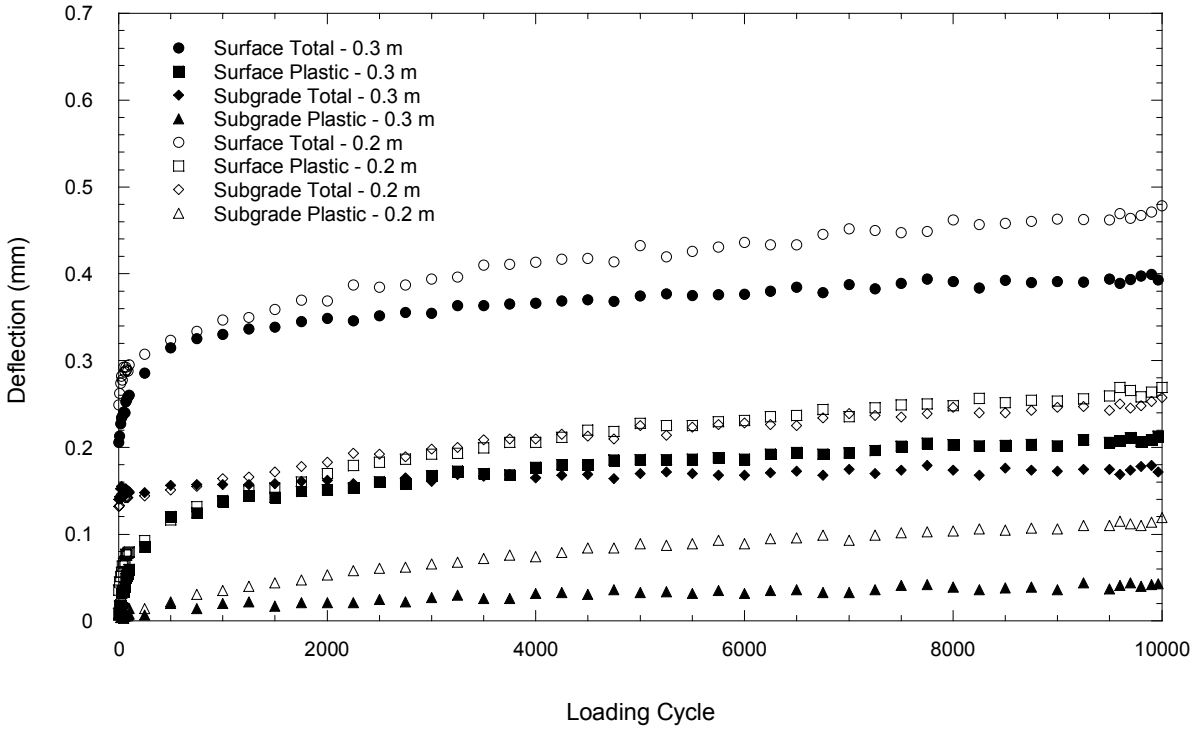

Fig. 4.3. Total and plastic deflection of surface and subgrade layers vs. number of loading cycles for blended RCA/Class 5.

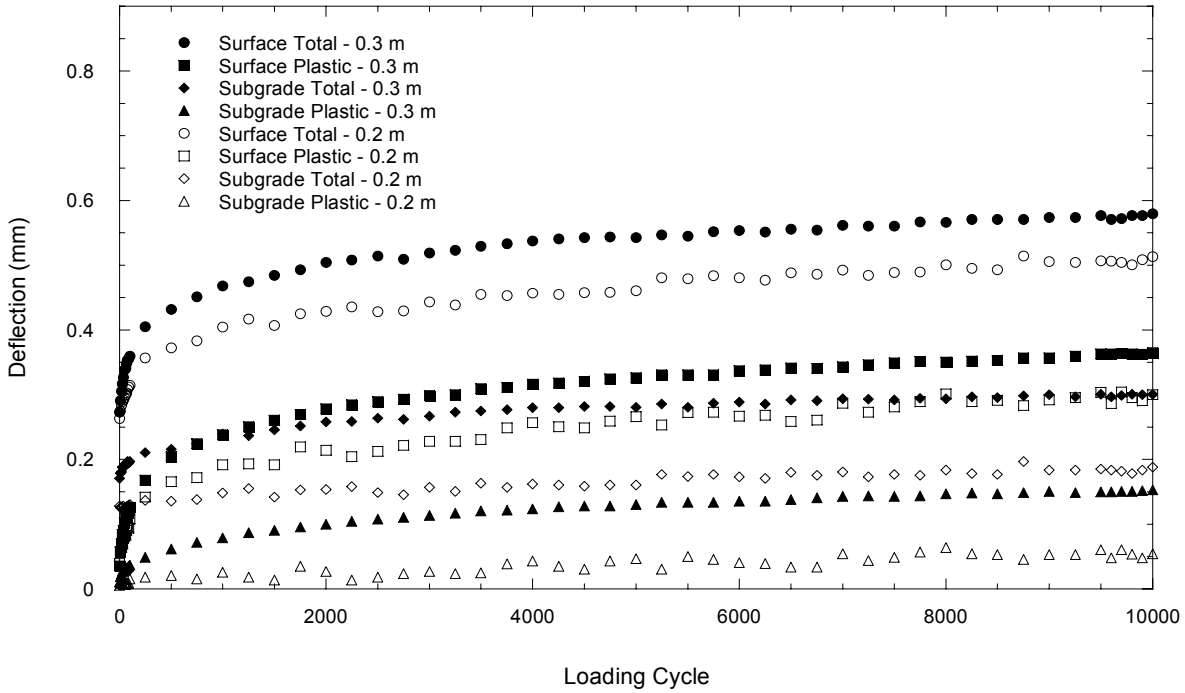

Fig. 4.4. Total and plastic deflection of surface and subgrade layers vs. number of loading cycles for Class 5.

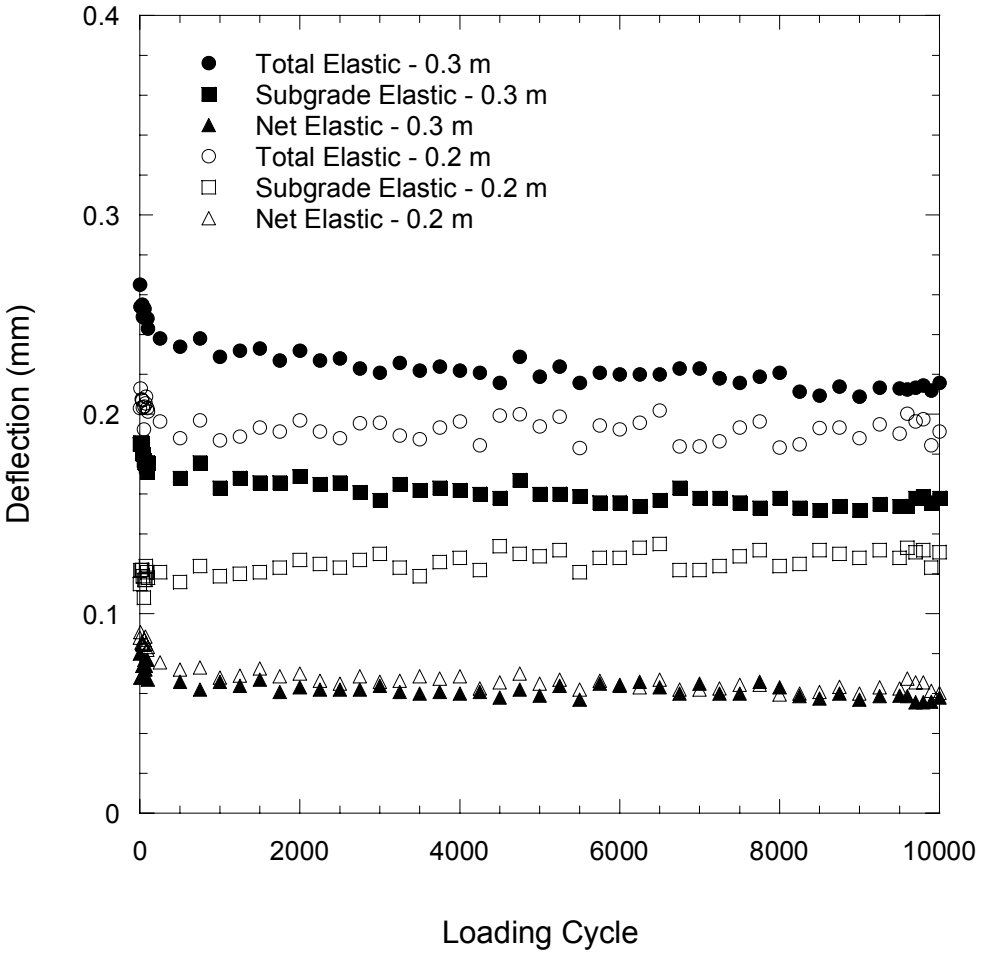

Fig. 4.5. Surface (total), subgrade, and net elastic deflection vs. number of loading cycles for RAP.

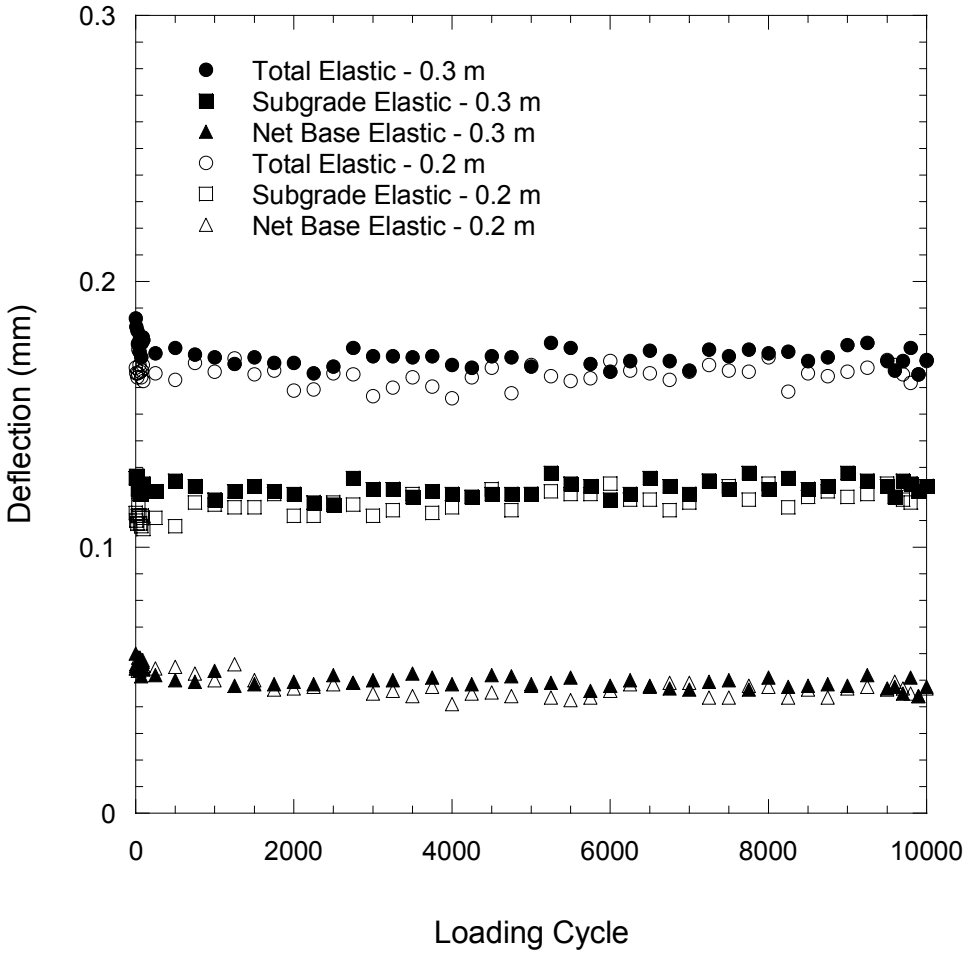

Fig. 4.6. Surface (total), subgrade, and net elastic deflection vs. number of loading cycles for RCA.

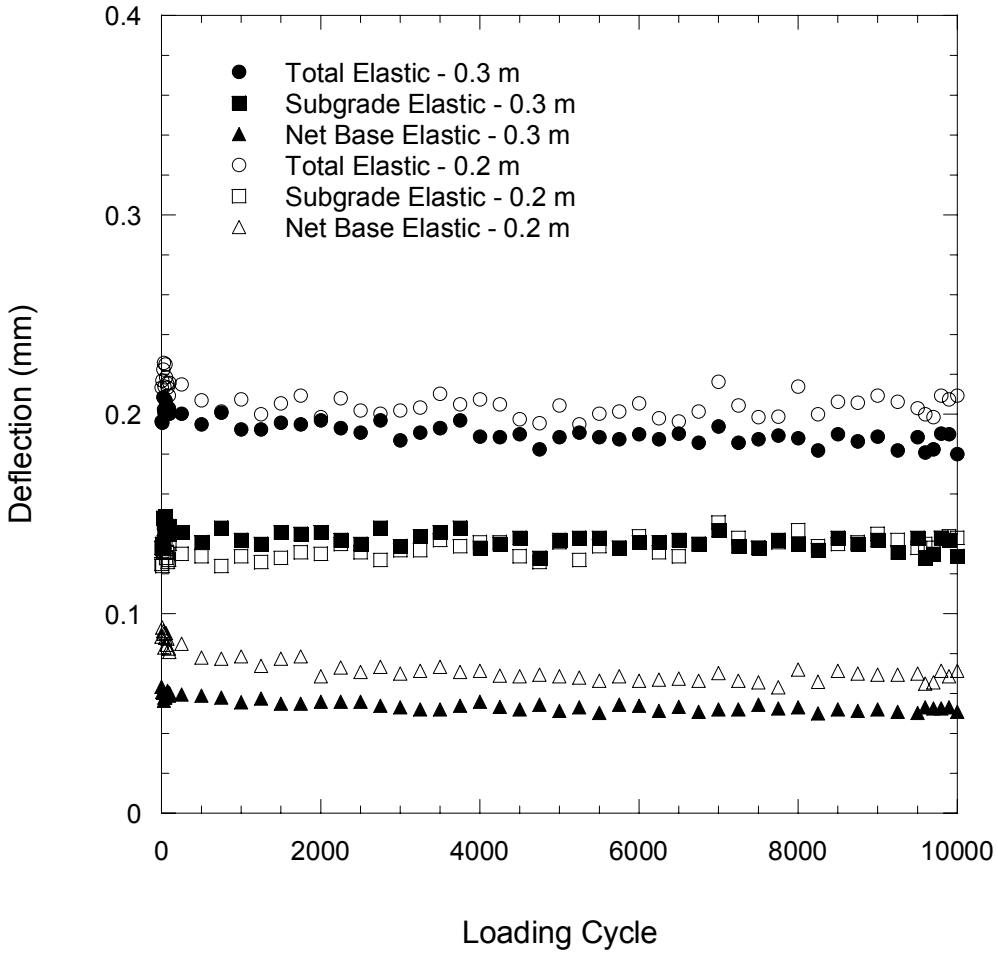

Fig. 4.7. Surface (total), subgrade, and net elastic deflection vs. number of loading cycles for blended RCA/Class 5.

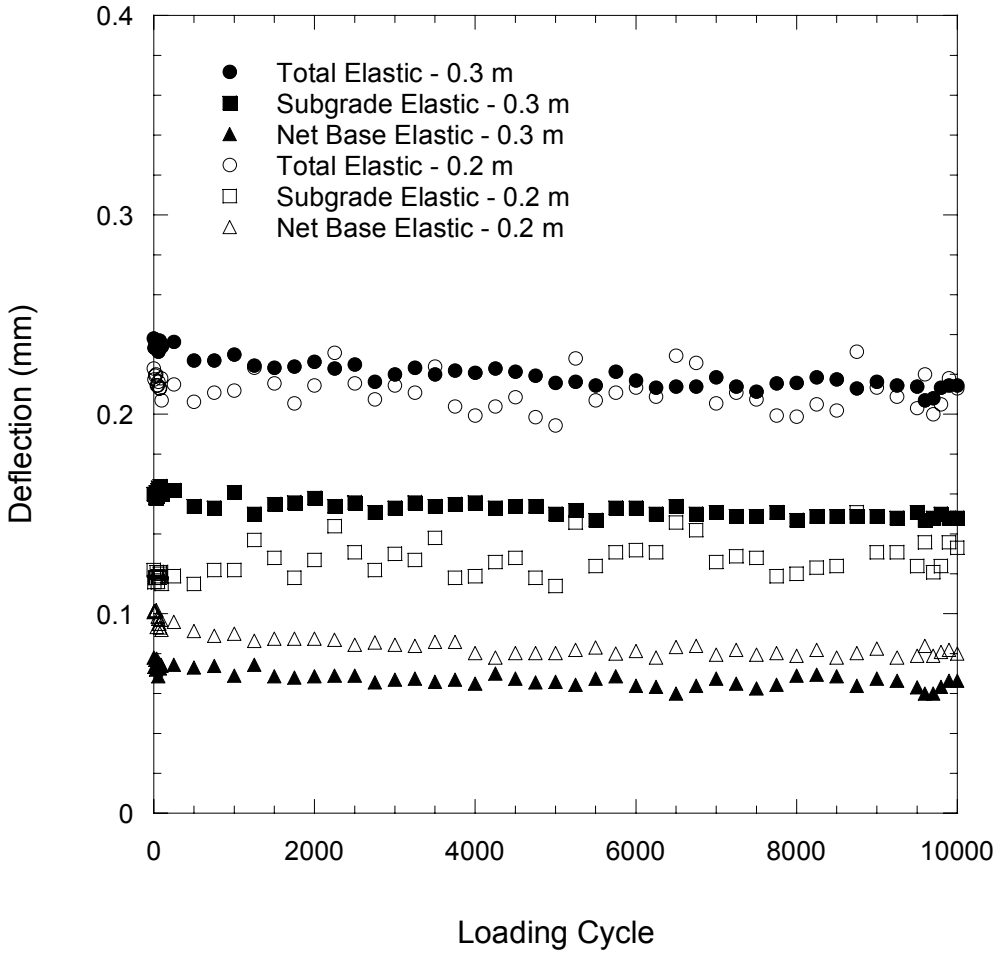

Fig. 4.8. Surface (total), subgrade, and net elastic deflection vs. number of loading cycles for Class 5.

stress within the layer more thoroughly, and therefore the amount of strain experienced in the material can be expected to be reduced. The subgrade elastic deflection was nearly constant during the loading of both layer thicknesses for each base course material.

A comparison of the surface and subgrade deflections after 10,000 loading cycles for 0.2-m and 0.3-m thick layers of RAP, RCA, blended RCA/Class 5 and Class 5 is presented in Fig. 4.9. The net plastic deflection is the difference between the total plastic deflection measured at the surface and the plastic deflection measured at the subgrade. The sum of the deflections represented in Fig. 4.9 is equal to the total deflection measured at the surface of the LSME at the end of loading. RAP and RCA had the largest and smallest amount of both total and net base plastic deflection, respectively, with Class 5 and blended RCA/Class 5 having the second and third largest amounts of both total and net base plastic deflections, respectively. The plastic deflection experienced by the RAP was approximately 211% and 402% greater than that of Class 5 for 0.2 m and 0.3 m layer thicknesses, respectively, whereas the plastic deflection experienced by the RCA was approximately 69% smaller than the plastic deflection experienced by the Class 5 for both layer thicknesses. The blended RCA/Class 5 material experienced plastic deflections that were 39% and 20% smaller than Class 5 for layer thicknesses of 0.2 m and 0.3 m, respectively. The net elastic and plastic deflections for 0.2 m and 0.3-m layer thicknesses of RAP, RCA, blended RCA/Class 5, and Class 5 can be compared in Fig. 4.10.

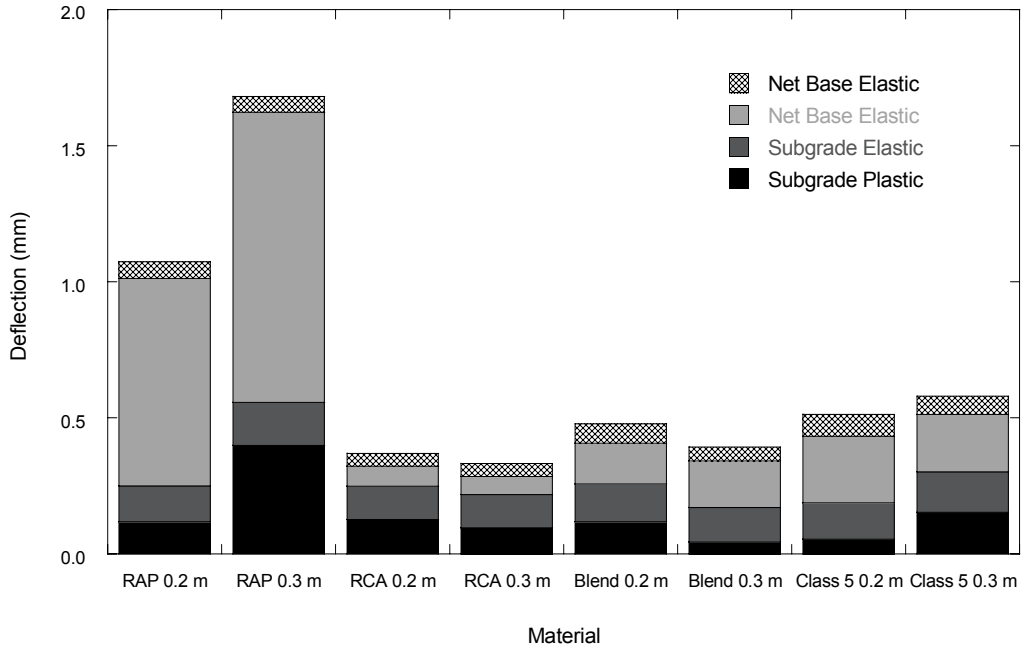

Fig. 4.9. Comparison of surface and subgrade deflections for RAP, RCA, blended RCA/Class 5, and Class 5.

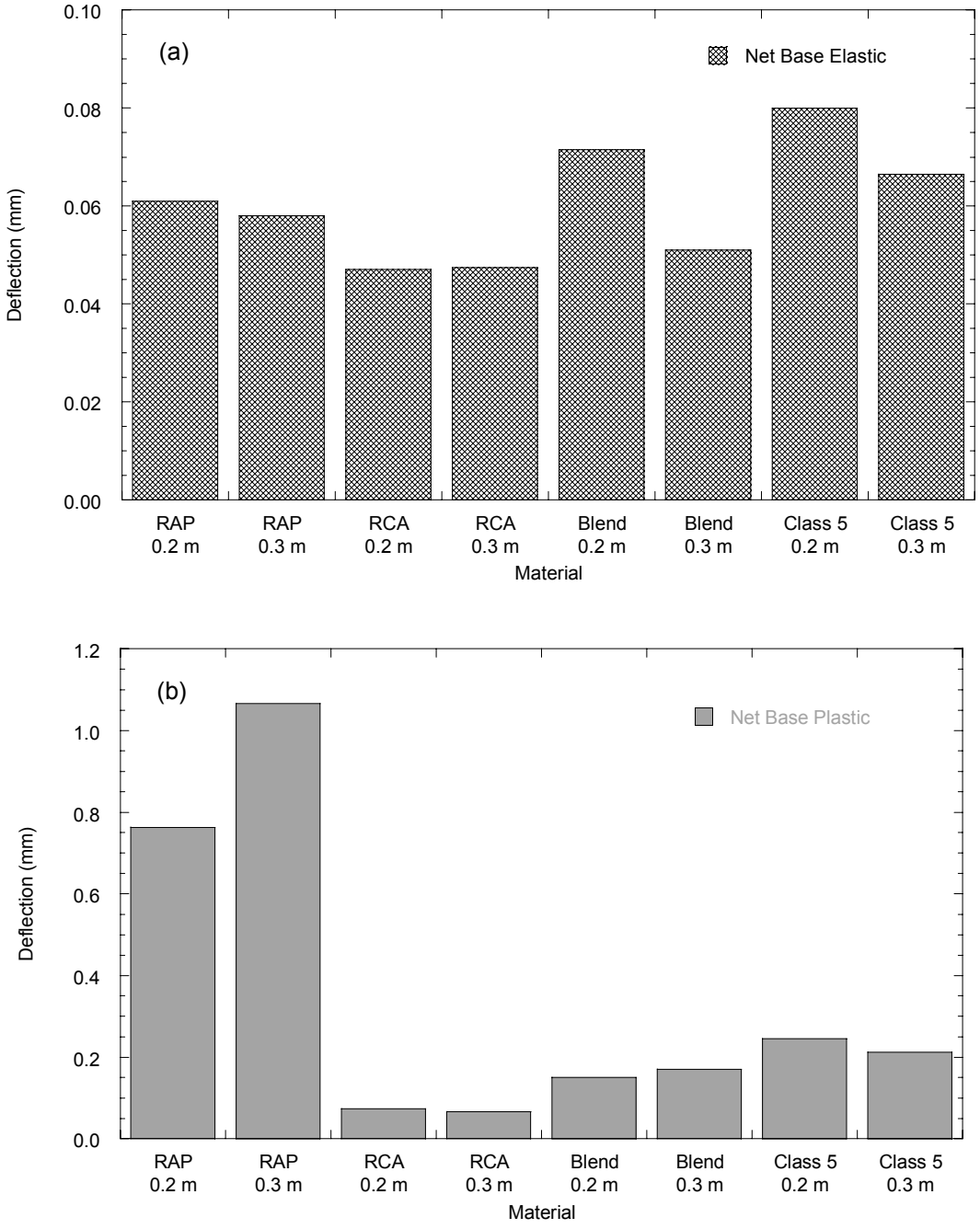

Fig. 4.10. Comparison of (a) net elastic and (b) net plastic deflections for RAP, RCA, blended RCA/Class 5, and Class 5.

The base plastic deflection of RCA and Class 5 was larger for the 0.2 m layer thickness compared to the 0.3 m layer thickness. Stress is better distributed within a layer of larger thickness, and the corresponding reduction in strain correlates to a reduction in plastic deflection. The plastic deflection of RCA and Class 5 decreased 10% and 13%, respectively, for an increase in layer thickness from 0.2 m to 0.3 m.

The plastic deflection experienced by the 0.3-m layer thickness of blended RCA/Class 5 is 13% larger than the plastic deflection experienced by the 0.2 m layer thickness, which contradicts the deflection that would be expected considering the deflections experienced by RCA and Class 5 alone. The most likely cause for this seemingly contradictory behavior is experimental error. Although LSME compaction was checked with a nuclear density gauge prior to testing, there is a possibility that the material directly under the loading plate was undercompacted. Undercompacted material would experience excess plastic deflection during the 10,000 cycles of loading, which would contribute to the total overall deflection. The effect of this undercompaction would be minimal for elastic deflection, however, as the compaction level required for the material to perform as linear-elastic would remain the same and would be achieved before the termination of loading.

The plastic deflection of RAP is 40% larger for the 0.3-m layer thickness compared to the 0.2-m layer thickness. This is attributed to the viscous nature of the asphalt coating on the RAP particles that contributes to increased amount of deflection of the layer despite the reduction of stress in the larger layer thickness.

The elastic and plastic net base deflection as a function of RCA content is presented in Fig. 4.11 for 0.2 m and 0.3 m layer thicknesses of RCA, blended

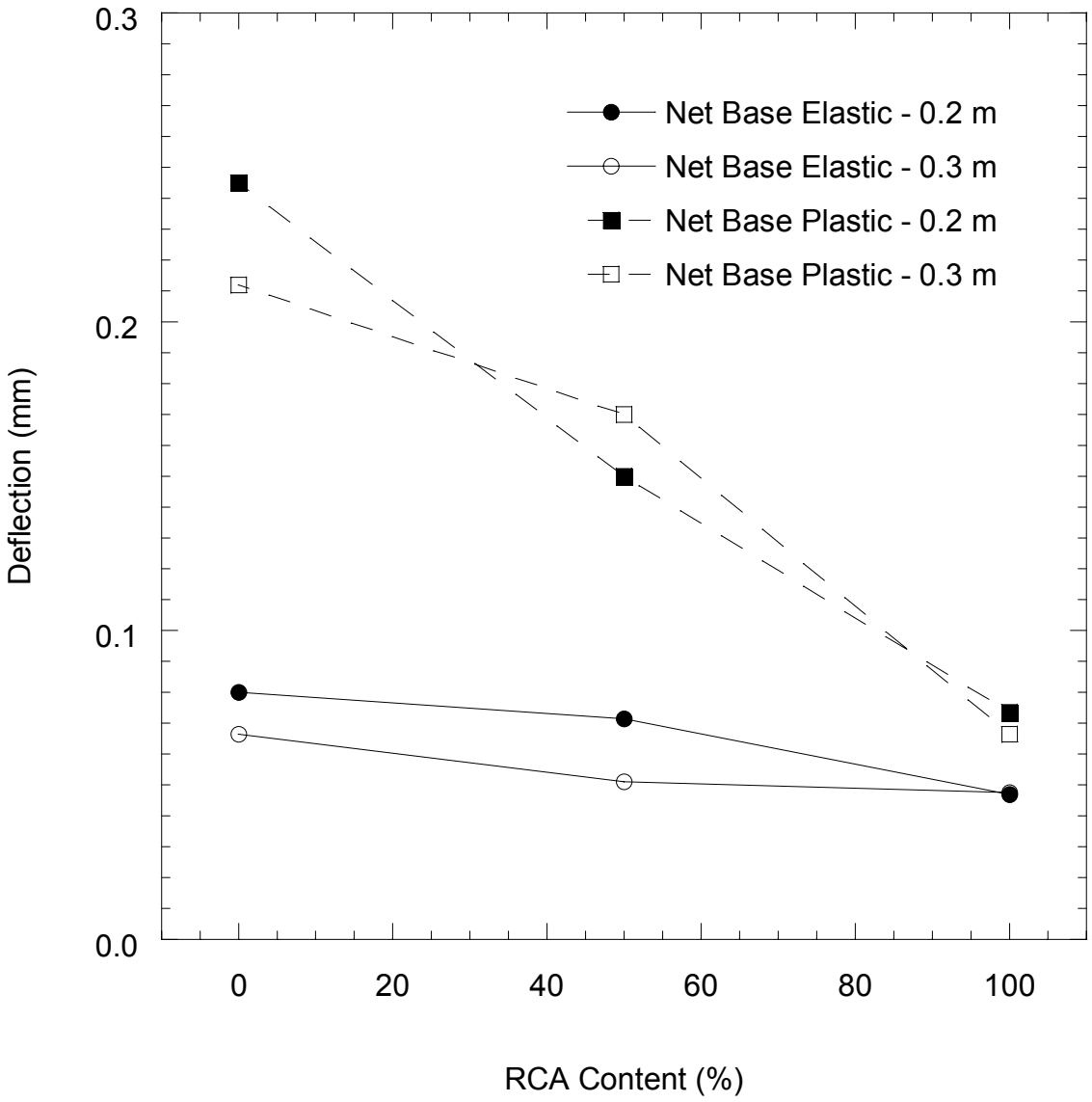

Fig. 4.11. Comparison of net base elastic and net base plastic deflections vs. RCA content for RCA, blended RCA/Class 5, and Class 5.

RCA/Class 5, and Class 5. The elastic deflection decreased slightly with an increase in RCA content, i.e., the 0.2-m and 0.3-m thick layers showed an overall decrease in the elastic deflections, i.e., approximately 0.03 mm and 0.02 mm, respectively. The plastic deflection also decreased with an increase in RCA content, although at a much higher rate. The 0.2-m and 0.3-m thick layers showed an overall decrease in plastic deflection of approximately 0.17 mm and 0.15 mm, respectively. As the RCA content increases, the elastic and plastic deflections of the different layer thicknesses seem to converge on common values, i.e., the elastic and plastic deflection of 100% RCA is approximately 0.05 mm and 0.07 mm, respectively, for both 0.2 m and 0.3 m layer thicknesses.

The average plastic strain (ε_p) in each base layer can be defined as:

$$\varepsilon_p = \frac{d_p}{t} \times 100 \qquad (4.1)$$

where d_p is the plastic deflection within the base layer and t is the layer thickness. The plastic strain of the base course as a function of loading cycle is presented in Figs. 4.12 thru 4.15 for 0.2-m and 0.3-m layer thicknesses of RAP, RCA, blended RCA/Class 5, and Class 5. The average plastic strain experienced by the 0.3-m thick base layer is greater than that experienced by the 0.2-m thick base layer for each of the tested materials. In addition, each material reaches a steady state condition within 500 cycles for both layer thicknesses.

The steady state condition achieved for RCA, blended RCA/Class 5, and Class 5 maintains a constant plastic strain rate of approximately zero, corresponding to a behavior, which is in accordance with plastic shakedown (Khogali et al. 2004,

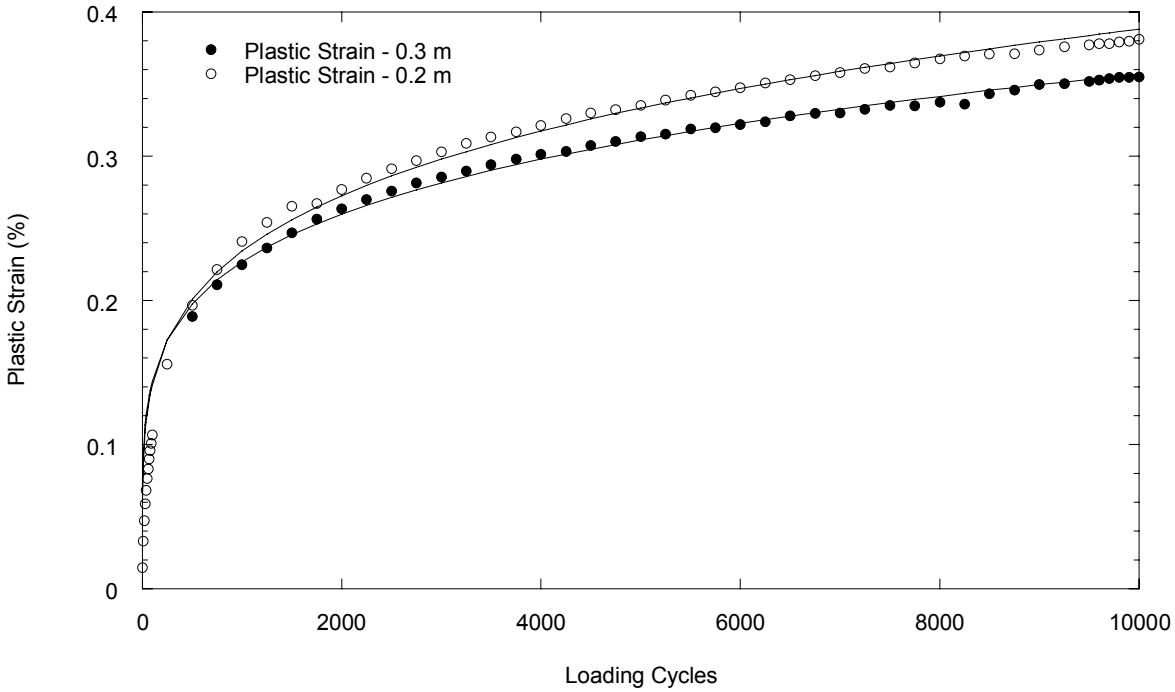

Fig. 4.12. Plastic strain vs. loading cycle for RAP.

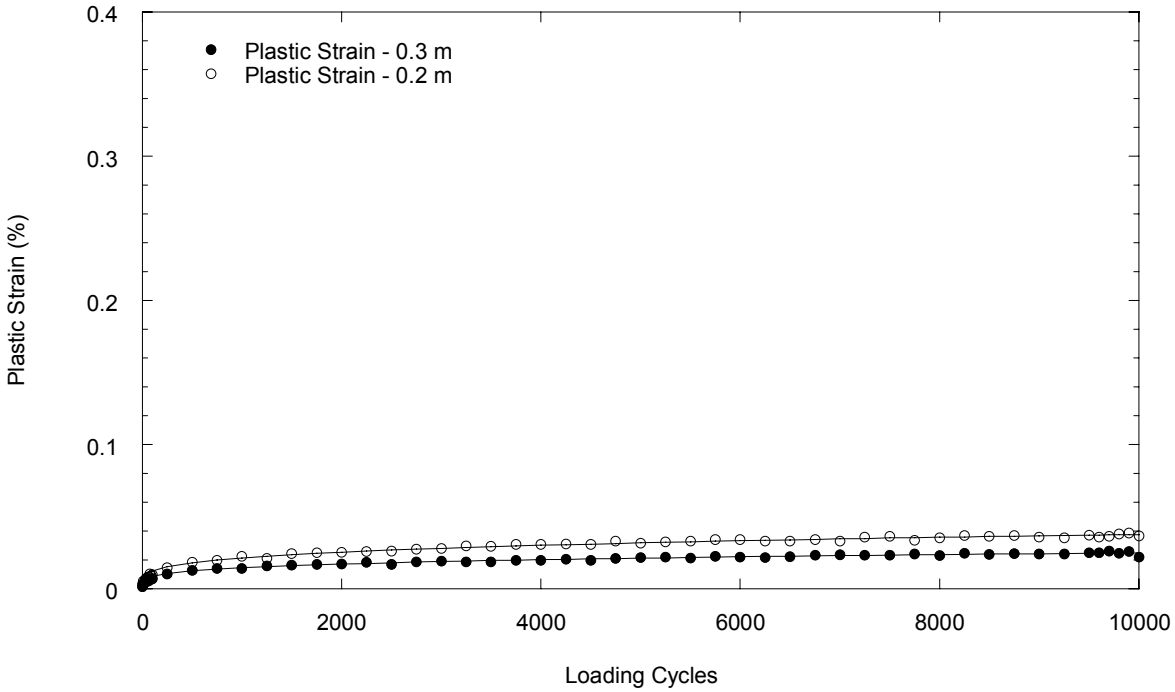

Fig. 4.13. Plastic strain vs. loading cycle for RCA.

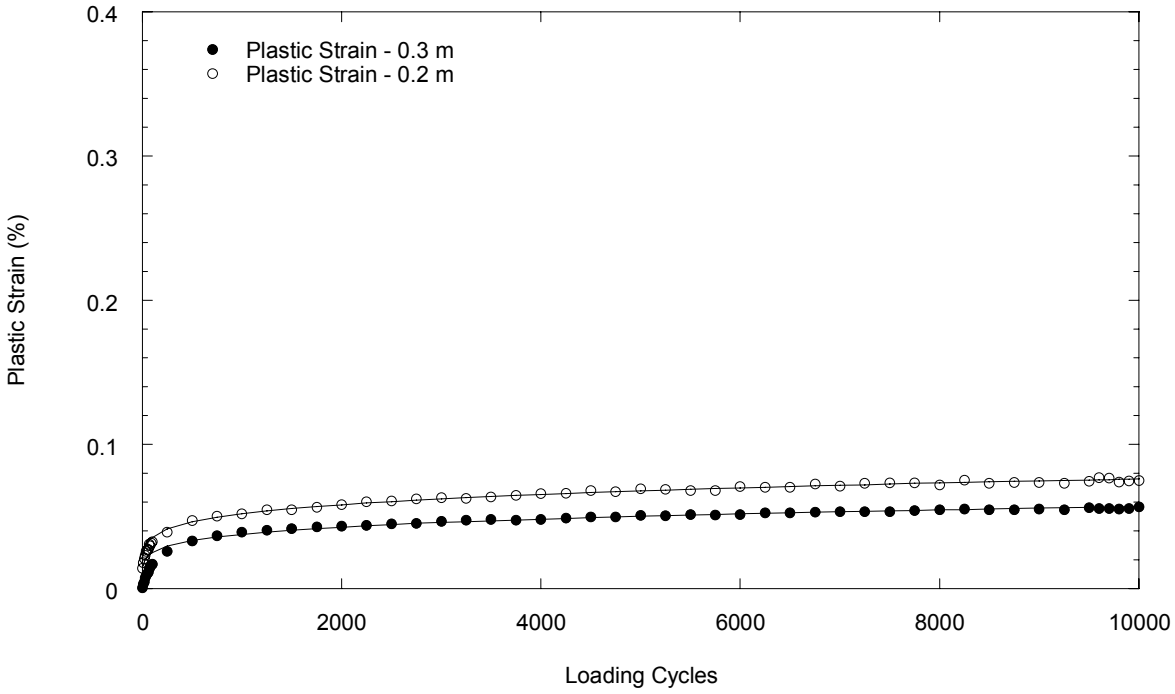

Fig. 4.14. Plastic strain vs. loading cycle for blended RCA/Class 5.

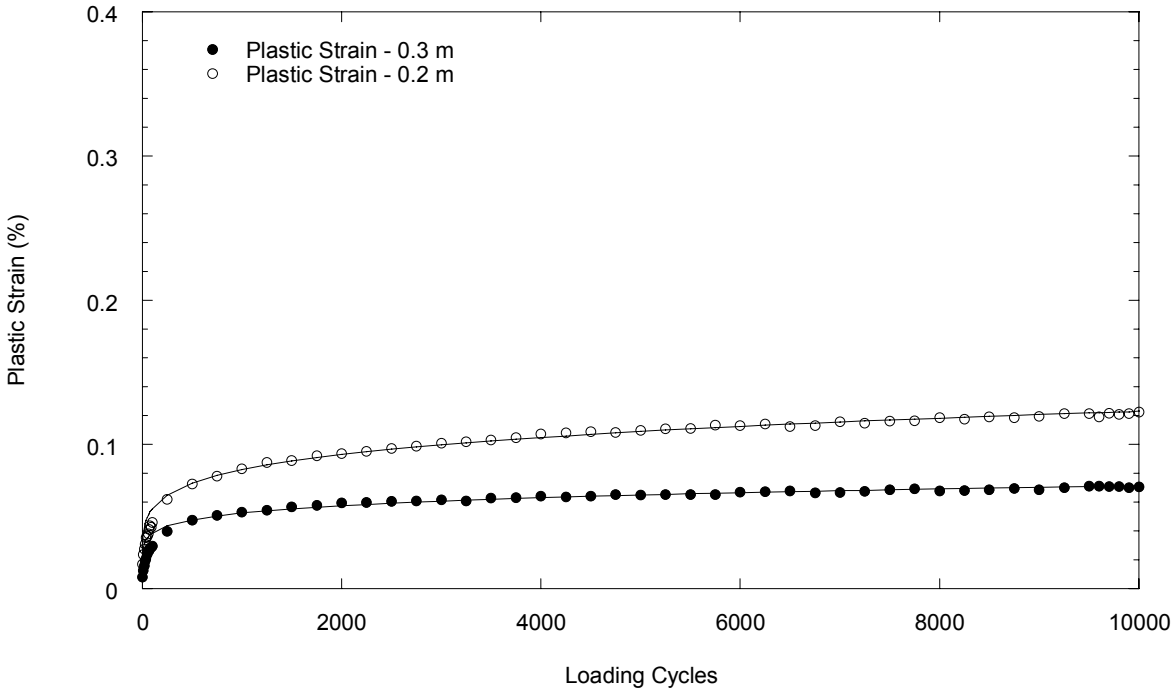

Fig. 4.15. Plastic strain vs. loading cycle for Class 5.

Yang et al. 2008, Kootstra et al. 2010). The steady state condition achieved for RAP also maintains a constant plastic strain rate; however the strain rate is non-zero and continues to accumulate with increased cyclical loading. The non-zero plastic strain rate in RAP can be attributed to the viscous nature of the asphalt that coats the RAP aggregate, and corresponds to behavior in accordance with creep shakedown (Mohammad et al. 2006, Kootstra et al. 2010).

The strain data from the LSME tests was fitted to the VESYS power function model (FHWA 1978) to estimate rutting potential. The VESYS power function is defined by:

$$\varepsilon_p = aN^b \qquad (4.2)$$

where a represents the initial densification after the first pass of traffic, b represents the rate at which permanent strain accumulates, and N is the number of load repetitions. Parameters a and b are dimensionless. The fitting parameters used in Eq. 4.2 are summarized in Table 4.1. The cumulative plastic strain in each of the base courses after $3x10^7$ loading cycles (i.e. 4000 daily truck loads over 20 years) was estimated using Eq. 4.2. Rutting depths based on the estimated plastic strain are also summarized in Table 4.1.

An acceptable limit to the rutting of flexible pavements has been suggested to be 13 mm (Huang, 2004). Based on LSME data, conventional granular base course (Class 5) can be expected to contribute 4 to 8% of the permissible rut depth. RCA and blended RCA/Class 5 can be expected to contribute 3 to 6% of the permissible rut depth, which is comparable to that of Class 5. Conversely, RAP can be expected

Table 4.1. Summary Resilient Modulus (SRM) and power model fitting parameters k1 and k2 Eq. 2.2) for base materials.

Material	Thickness (m)	Eq. 4.x		ε_p (%) due to cyclic load for $N=3x10^7$	Rutting depth due to plastic strain in base (mm)
		a	b		
RAP	0.2	0.051	0.220	2.25	4.5
	0.3	0.058	0.197	1.72	5.2
RCA	0.2	0.004	0.243	0.26	0.5
	0.3	0.003	0.230	0.16	0.5
Blend	0.2	0.017	0.165	0.29	0.6
	0.3	0.011	0.178	0.24	0.7
Class 5	0.2	0.025	0.173	0.49	1.0
	0.3	0.021	0.134	0.21	0.6

to contribute between 30 and 40% of the acceptable rut depth, which is appreciable compared to that contributed by Class 5. Flexible pavements that incorporate RAP as a base course layer can be expected to encounter excessive rutting, whereas flexible pavements that incorporate RCA and RCA/natural aggregate blends will experience rutting comparable to pavements incorporating conventional base course aggregate.

4.2. Comparison of Large and Small-Scale Resilient Moduli

The resilient modulus as a function of bulk stress for RAP, RCA, blended RCA/Class 5, and Class 5 are presented in Figs. 4.16 thru 4.19, respectively. This relationship is presented for both the 0.2 m and 0.3 m thick layers tested in the LSME, as well as for the bench-scale specimen tests performed according to NCHRP 1-28a on the same materials by Son (2010). Bench-scale tests were evaluated for deflections measured externally, relative to the test cell, and internally at the upper and lower quarter points along the specimen length. Fitting parameters k_1 and k_2 determined from the bench-scale tests were used to calculate the resilient modulus as a function of bulk stress as defined by the power function model suggested by Eq. 2.2. The parameter k_2 determined from the bench-scale tests was used in the back analysis of the LSME data to determine the parameter k_1 that allowed the matching of the measured deflections in the LSME using the MICHPAVE code with the modulus function according to Eq. 2.2. The power-function relationship illustrates the concept that increased bulk stress contributes to an increase in resilient modulus for granular materials. A summary of the k_1 and k_2

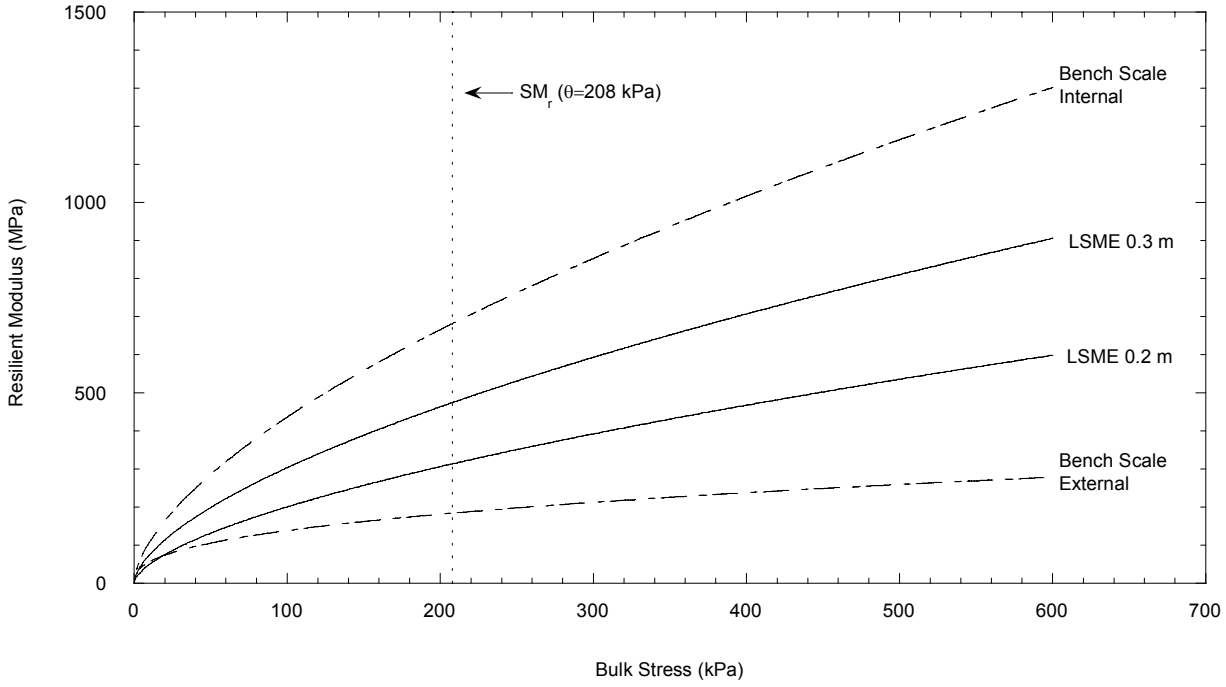

Fig. 4.16. Resilient modulus vs. bulk stress for bench-scale and LSME test methods for RAP.

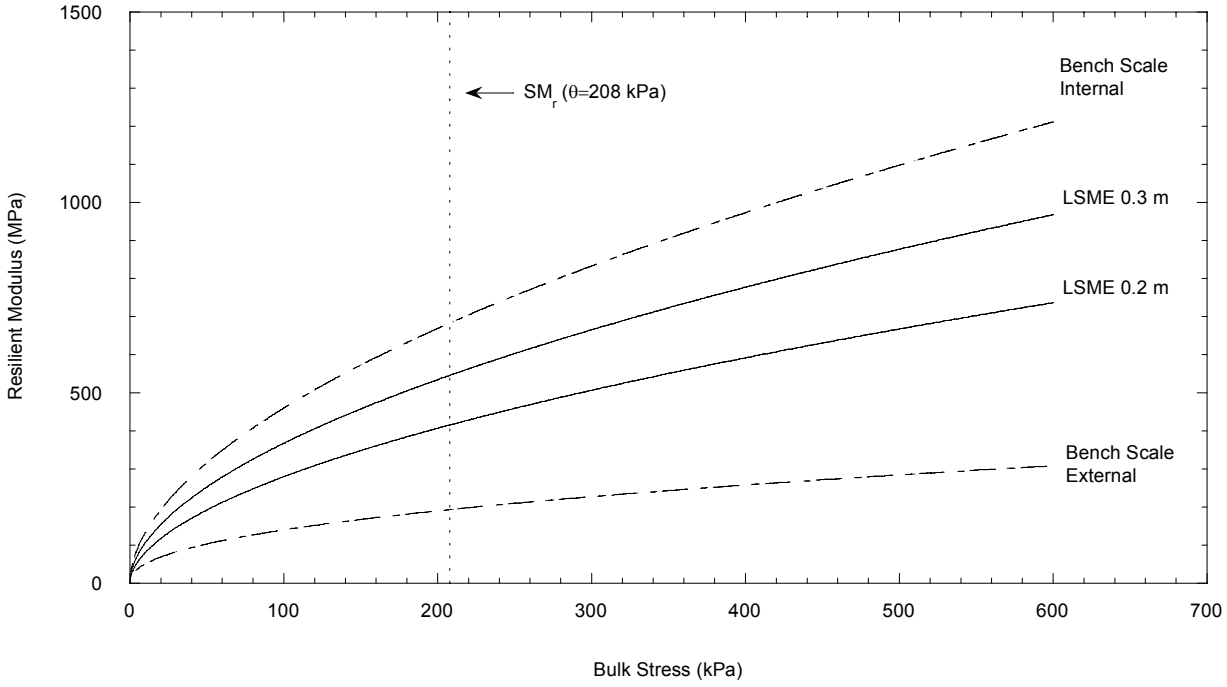

Fig. 4.17. Resilient modulus vs. bulk stress for bench-scale and LSME test methods for RCA.

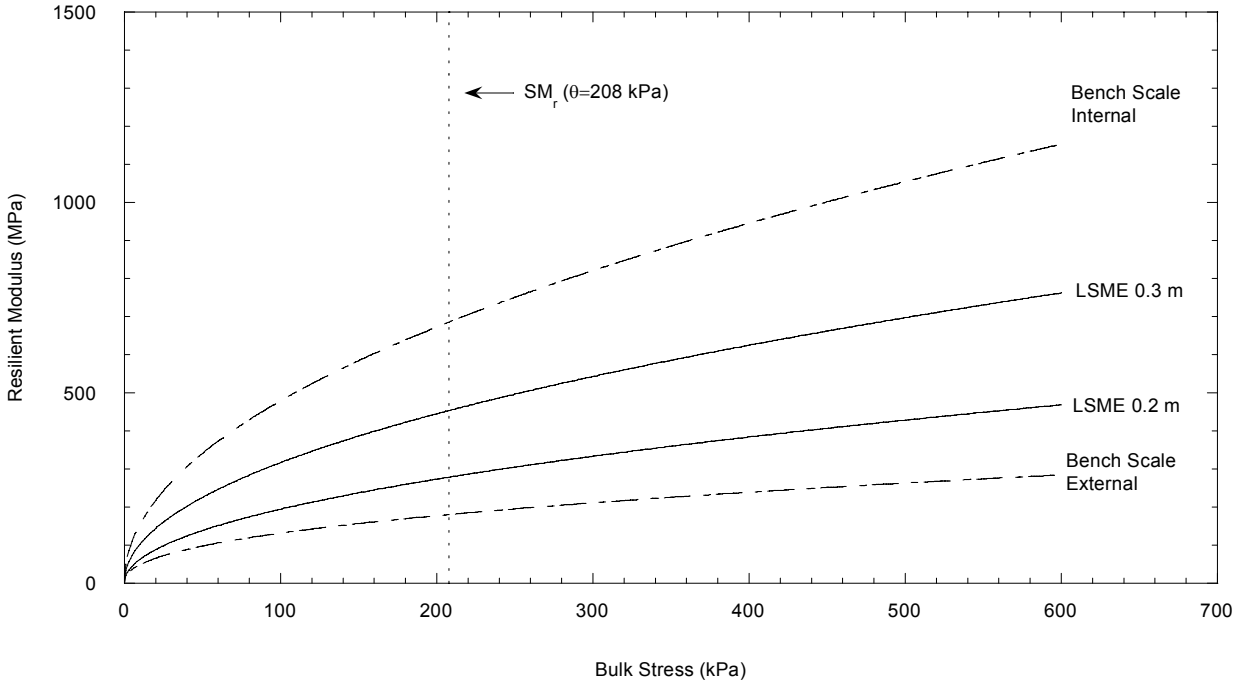

Fig. 4.18. Resilient modulus vs. bulk stress for bench-scale and LSME test methods for blended RCA/Class 5.

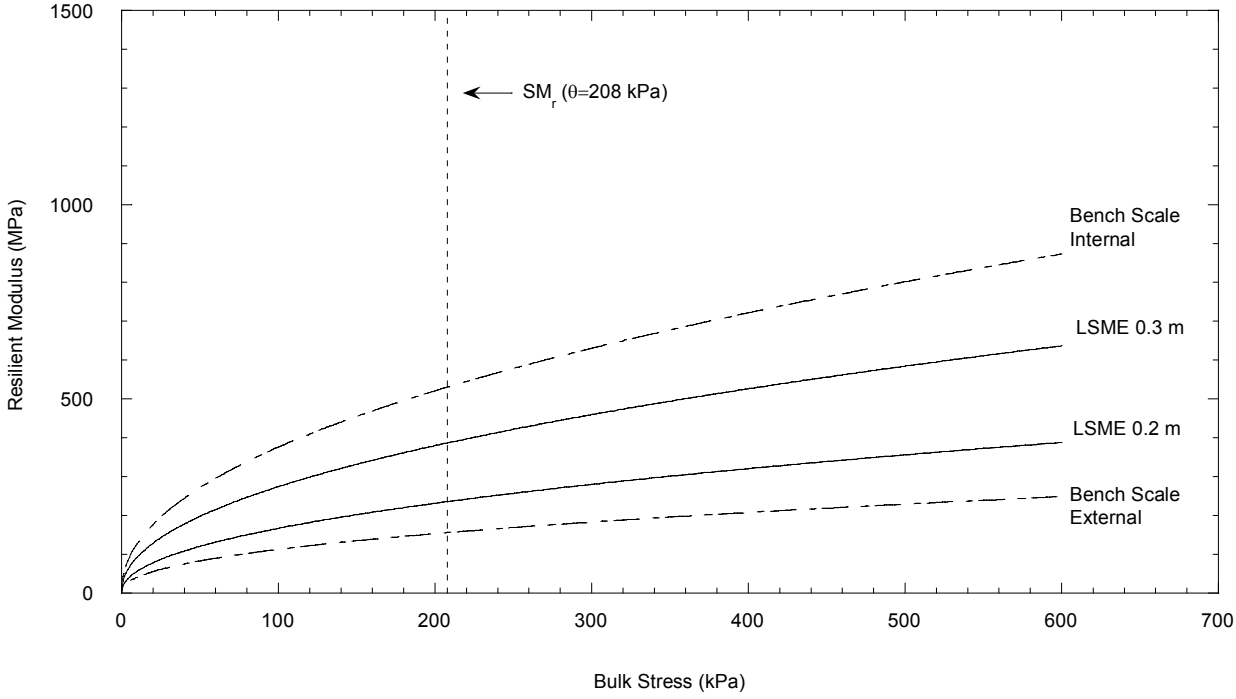

Fig. 4.19. Resilient modulus vs. bulk stress for bench-scale and LSME test methods for Class 5.

obtained in the tests is presented in Table 4.2.

The internal and external bench-scale tests had the highest and lowest resilient modulus, respectively, and the LSME tests for 0.3 m and 0.2 m layer thicknesses had the second and third highest resilient modulus, respectively, for each of the four materials (Figs. 4.16-4.19). No direct correlation can be made between the resilient moduli measured for bench-scale tests and the resilient modulus back-calculated from the LSME. The magnitudes of the four tests appear to be evenly spaced when referenced between the maximum and minimum values defined by the bench-scale tests. The moduli of both LSME tests seem to trend closer to the internal bench-scale test for the RCA case, and to the external bench-scale test for the blended RCA/Class 5 case; however these trends are slight and should not be considered direct correlations.

A comparison of the summary resilient moduli (SRM) determined for RAP, RCA, blended RCA/Class 5 and Class 5 are presented in Fig. 4.20. The SRM is based on a bulk stress of 208 kPa as suggested for base course materials by NCHRP 1-28a sec 10.3.3.9, and calculated according to Eq. 2.2 using the k_1 and k_2 presented in Table 4.2. The SRM calculated for each test method is also presented in Table 4.2.

RCA and Class 5 had the highest and lowest SRM, respectively, for each of the four testing methods. The SRMs of the RAP and blended RCA/Class 5 are approximately equal in magnitude for bench-scale testing, with RAP having a marginally higher SRM for both LSME tests. The SRM of RCA was 42% to 77% greater than that of Class 5, while the SRM of RAP was 23% to 33% greater. The

Table 4.2. Summary Resilient Modulus (SRM) and power model fitting parameters k1 and k2 Eq. 2.2) for base materials.

Material	Test Method	Thickness (m)	Measured Parameters		
			k1	k2	SRM (MPa)
RAP	Bench-Scale – Internal	0.30	26.3	0.61	674
	Bench-Scale – External	0.30	23.0	0.39	180
	LSME	0.20	12.1	0.61	314
		0.30	18.3	0.61	474
Class 5	Bench-Scale – Internal	0.30	43.2	0.47	525
	Bench-Scale – External	0.30	14.9	0.44	152
	LSME	0.20	19.2	0.47	236
		0.30	31.5	0.47	386
Blend	Bench-Scale – Internal	0.30	50.2	0.49	675
	Bench-Scale – External	0.30	18.2	0.43	182
	LSME	0.20	20.4	0.49	278
		0.30	33.2	0.49	454
RCA	Bench-Scale – Internal	0.30	38.3	0.54	680
	Bench-Scale – External	0.30	18.5	0.44	189
	LSME	0.20	23.3	0.54	417
		0.30	30.6	0.54	547

Note: SRM calculated at a bulk stress of 208 kPa.

* Bench-scale SRM reported by Son (2010).

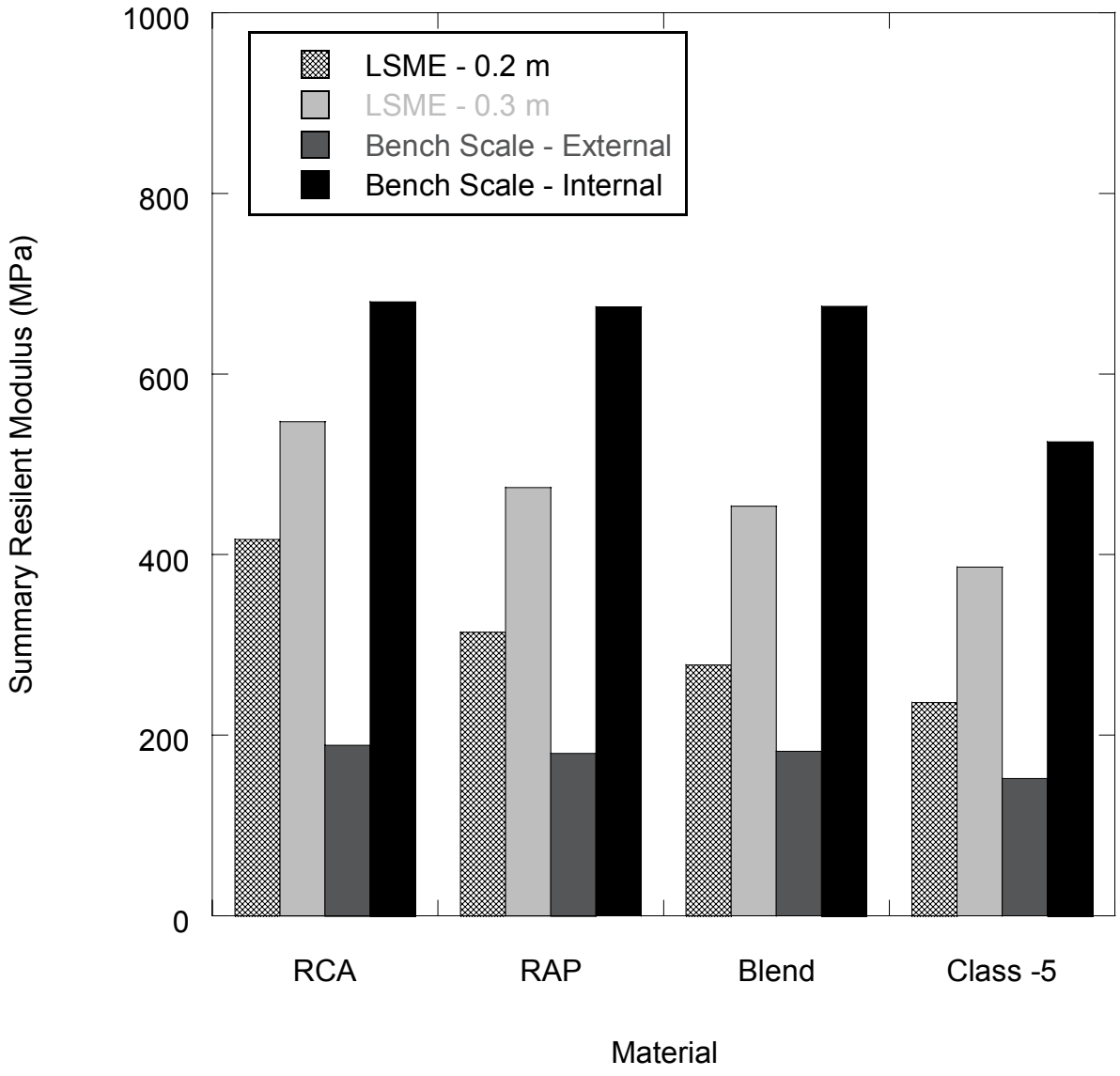

Fig. 4.20. Comparison of summary resilient modulus for RAP, RCA, blended RCA/Class 5, and Class 5.

SRM of the blended RCA/Class 5 was 18% greater than that of Class 5, which was comparable in magnitude to the SRM of RAP.

The SRM as a function of layer thickness is presented in Fig. 4.21 for RAP, RCA, blended RCA/Class 5, and Class 5. The resilient modulus of each material increases with a corresponding increase in layer thickness. The magnitude of this increase, which lies between 130 MPa and 176 MPa, appears relatively consistent for all materials and does not appear to trend differently for any individual material. The SRM as a function of RCA content is presented in Fig. 4.22 for RCA, blended RCA/Class 5, and Class 5. The SRM of the materials increases with an increase in RCA content. The magnitude of the increase seems to increase at the same rate regardless of layer thickness. The blended RCA/Class 5 defines a downward "spike" for both the 0.2 m and 0.3 m layer thicknesses, which interrupts an otherwise linear trend. One possible reason for this spike is that there is some form of particle interaction that is reducing the stiffness of the blended material as a whole. A second, more probable reason for the spike is that the blended material is not a perfect blend of 50% RCA and 50% Class 5. Measuring the mass of materials in the field relies on approximations to a certain extent, and the actual amounts blended together might vary depending on the experience of the field engineer. Also, the material was mixed in the field using the blade of a bulldozer. Such mixing methods are not thorough, and samples taken from such mixtures could vary depending on sample location. Based on these assumptions and the SRM calculated for the blended material, a blend incorporating an RCA content of between 20% and 40% would better fit a linear trend between SRMs calculated for 0% and 100% RCA.

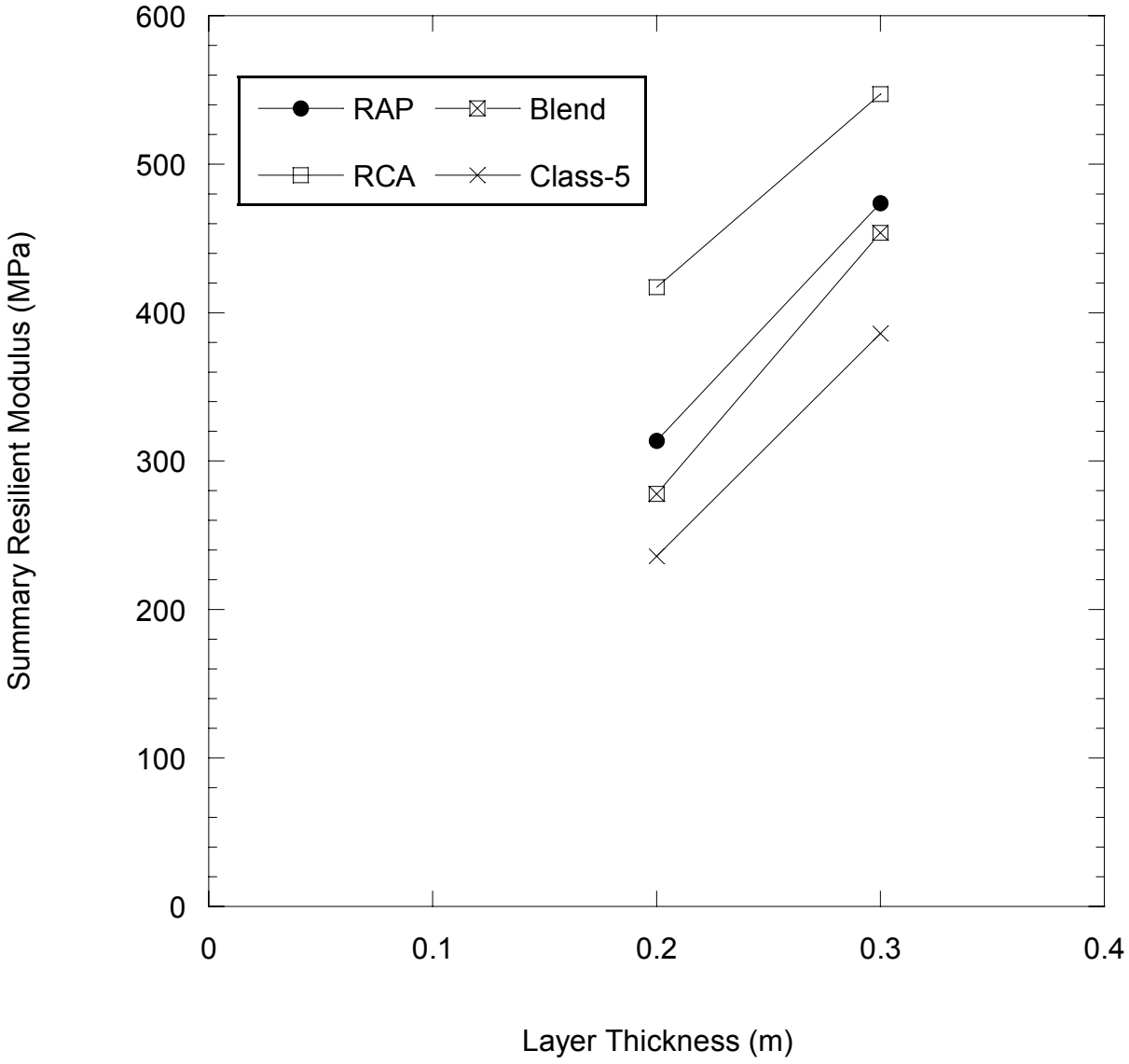

Fig. 4.21. Summary Resilient Modulus vs. layer thickness for RAP, RCA, blended RCA/Class 5, and Class 5.

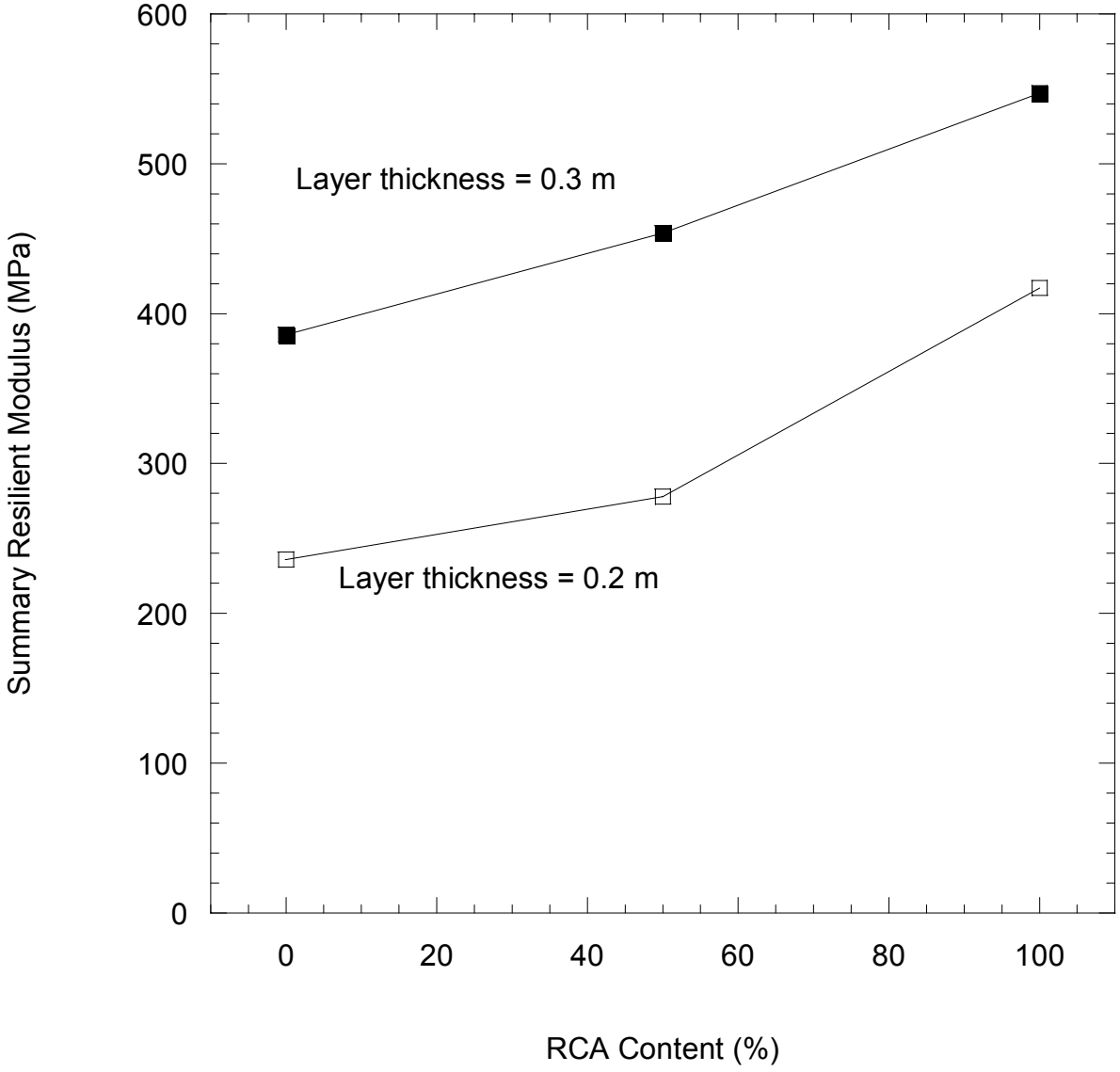

Fig. 4.22. Summary Resilient Modulus vs. RCA content for RCA, blended RCA/Class 5, and Class 5.

4.3. Scaling Laboratory Results to Field Conditions

4.3.1. Background

The elastic modulus of granular material has been shown to be sensitive to strain amplitude (Seed and Idriss 1970, Hardin and Drnevich 1972, Edil and Luh 1978). Thicker layers distribute stress more efficiently and reduce the amount of strain experienced by the material. The resilient modulus of a material evaluated at a given bulk stress can vary in magnitude depending on which testing method is being used (Fig. 4.20). These differences in magnitude are assumed to be due to differences in stress state and strain level (Tanyu et al. 2003, Schuettpelz et al. 2008, Benson et al. 2009). A more accurate comparison between the various testing methods can be established by adjusting the resilient modulus to account for these differences in stress and strain level.

A backbone curve can be used to describe the stress-strain dependency of resilient modulus (Seed and Idriss 1970, Hardin and Drnevich 1972). Backbone curves represent the ratio of shear modulus (G_γ) at a given shear strain to the low-strain shear modulus (G_{max}) as a function of shear strain amplitude for a given state of stress. The relation between shear modulus and shear strain can be approximated by the following relationship suggested by Hardin and Drnevich:

$$\frac{G_\gamma}{G_{max}} = \frac{M_r}{E_s} = \frac{1}{1+\gamma_h} \tag{4.3}$$

where γ_h is defined as the hyperbolic strain. The hyperbolic strain is the strain normalized with respect to the reference strain (γ_r):

$$\gamma_h = \frac{\gamma}{\gamma_r}\left[1+ae^{-b\left(\frac{\gamma}{\gamma_r}\right)}\right] \tag{4.4}$$

where a and b describe the shape of the backbone curve. The reference strain is defined as the strain at the intersection of maximum shear stress and shear modulus (Hardin and Drnevich 1972). These relationships can be used for resilient modulus dependency on strain amplitude by assuming that the ratio G_γ/G_{max} is equal to the ratio of resilient modulus at a given shear strain to the low-strain Young's modulus (maximum modulus) (M_r/E_s),

4.3.2. Measurement of Low-strain Modulus

The low-strain modulus of the materials was determined using the small-scale simple seismic test method suggested by Schuettpelz (2009). The method is based on the propagation of surface waves and is intended to be a much simpler method of data acquisition when compared to methods involving larger testing schemes. Material was compacted to 95% of the maximum dry density under modified compaction effort within a 5-gallon bucket to a volume of approximately $11x10^{-3}$ m^3. Approximately 0.23 kN of material was used for each test (Fig. 4.23). Material was compacted with a tamper in four lifts of equal measure to ensure uniform density. A 150 mm diameter load plate was placed central to the surface of the material, and a small amount of material was removed from opposing sides of the plate. Two accelerometers were placed adjacent to the plate and buried approximately 10 mm below the soil surface. The accelerometers were aligned with one axis parallel to the ground surface, and 500 gram masses were used to seat the accelerometers into the soil and make the first arrivals of elastic waves more distinguishable. The

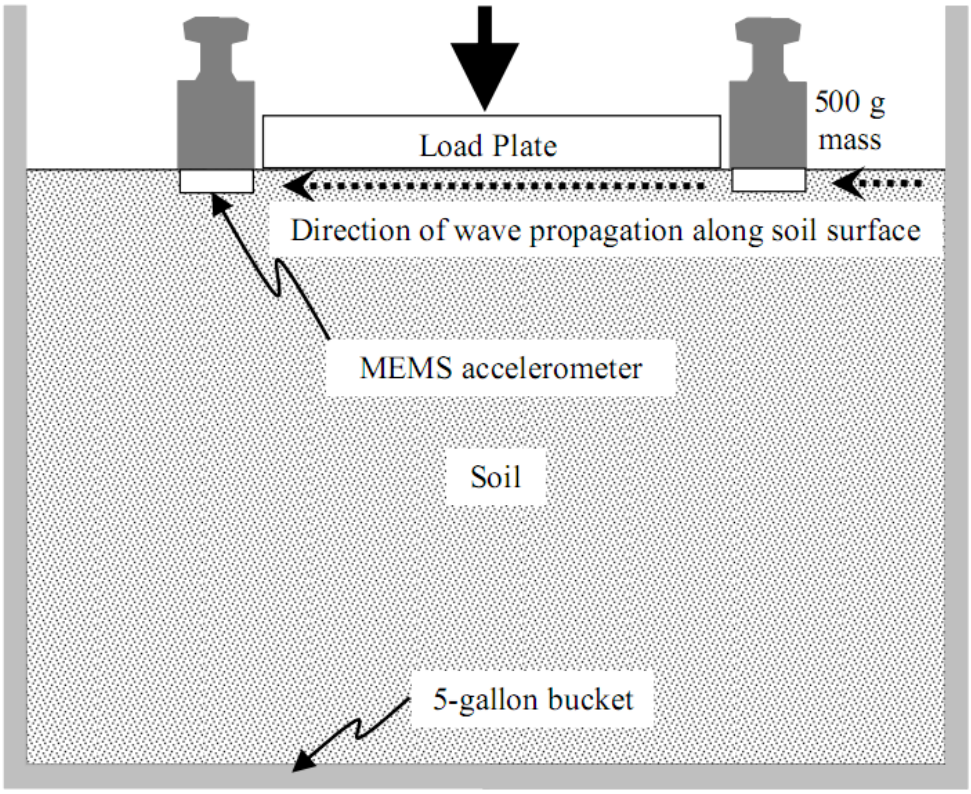

Fig. 4.23. Simplified test setup to determine low-strain constraint modulus with applied stress near the surface. (Adapted from Edil and Fratta 2009)

final distance between the accelerometers was recorded for each test. The actuator from the LSME was used to apply varying static loads to the material during testing.

The side of the 5-gallon bucket was tapped with a rubber mallet and the travel time of the surface wave between the two accelerometers was recorded. The P-wave velocity (V_p) was determined by multiplying the surface velocity (V_r) by a conversion factor based on the Poisson's ratio (ν) (Santamarina et al. 2001, Kramer 1996):

$$V_p = V_r \frac{(1+\nu)\sqrt{\frac{2(1-\nu)}{1-2\nu}}}{0.874+1.117\nu} \tag{4.5}$$

V_p in particulate media is dependent on elastic modulus (E), Poisson's ratio (ν), and density (ρ) (Santamarina et al. 2001, Richart et al. 1970):

$$V_p = \sqrt{\frac{E(1-\nu)}{\rho(1+\nu)(1-2\nu)}} \tag{4.6}$$

The velocity of wave propagation increases with increasing applied load and soil stiffness.

The low-strain elastic modulus can be calculated from the V_p, ρ, and ν of the material by rearranging Eqn. 4.6:

$$E_s = \frac{V_p^2(1+\nu)(1-2\nu)}{(1-\nu)} \tag{4.7}$$

where ν was taken to be 0.35 for the granular material. The low-strain elastic modulus was plotted as a function of the stress applied to the surface of the soil by the loading plate. The low-strain elastic modulus was assumed to increase with the applied stress according to the power function described by Eqn. 2.2. The fitting parameters $k_{1,s}$ and $k_{2,s}$ were varied until a best-fit was found for the plotted data.

The relationship between E_s and the applied stress for the evaluated base course materials is presented in Fig. 4.24. The low-strain modulus determined for the RCA and blended material were of approximately the same magnitude, with the Class 5 having a low-strain modulus approximately two-thirds the magnitude of RCA and blended material. The low-strain modulus for the RAP was significantly higher of a magnitude approximately 3.5 to 5 times greater than the other materials. The asphalt coating the RAP is most likely self-adhering, and under small strains and the effects of this adhesion are not as easily overcome as the typical particle friction common in non-bituminous materials. This resistance to strain at the particle level would increase the low-strain modulus of the RAP accordingly.

4.3.3. Development of Backbone Curve

The backbone curve was developed from the resilient modulus and shear strain data collected from the bench-scale, LSME and FWD testing. Vertical strains and bulk stresses were determined for the bench-scale tests using NCHRP 1-28a, and for the LSME and FWD tests using MICHPAVE at varying depths within the base course layers. The shear strain was determined from the vertical strain (Kim and Stokoe 1992, Tanyu et al. 2003):

$$\gamma=\varepsilon(1+v) \qquad (4.8)$$

where γ is the shear strain, ε is the vertical strain, and v is the Poisson's ratio. The normalized resilient modulus was determined using Eqn. 4.9:

$$\text{Normalized resilient modulus}= \frac{M_r}{E_s} \qquad (4.9)$$

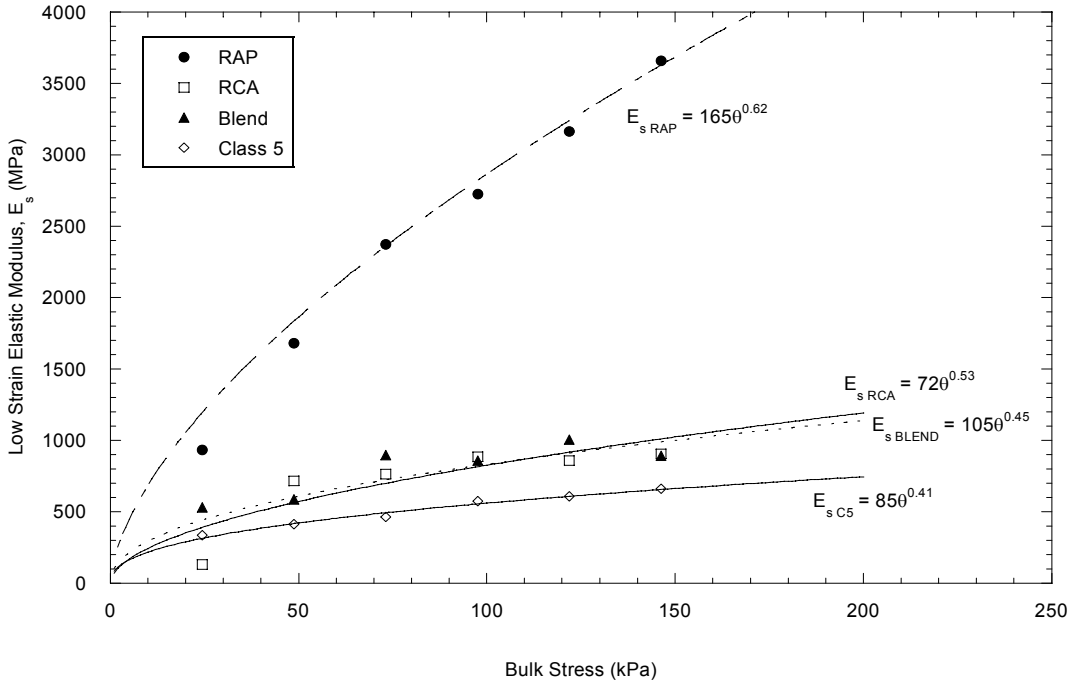

Fig. 4.24. Low-strain elastic modulus as a function of applied vertical stress.

where M_r and E_s are the resilient modulus and low-strain Young's modulus for a particular bulk stress, respectively. Parameters a and b in Eqn. 4.4 were adjusted to obtain a best-fit to the calculated points. The bulk stress, resilient modulus, low-strain Young's modulus, and normalized resilient modulus for each test method are presented in Table 4.3.

The backbone curves showing normalized modulus as a function of shear strain are shown in Figs. 4.25 thru 4.28 for RAP, RCA, Blended RCA/Class 5 and Class 5. The backbone shape describes the stress-strain behavior of the evaluated base course and is unique for a given material. The bench-scale tests with internally and externally measured deflections produce the lowest and highest strain levels, respectively. The 0.3-m and 0.2- m thick LSME tests produce the second and third lowest strains, respectively, with the FWD producing strains between those produced by the 0.2-m thick LSME and the external bench-scale test. The normalized resilient moduli of the RAP are considerably smaller compared to the normalized resilient modulus of the other tested materials. The bitumen coating the RAP causes the particles to adhere to each other, which leads to an increase in strain resistance at low stresses.

4.3.4. Scaling Specimen Tests to Field-Scale Conditions

A comparison of the resilient modulus calculated at field bulk stress is presented in Fig. 4.29 for RAP, RCA, blended RCA/Class 5, and Class 5. The field bulk stress is the bulk stress experienced under FWD loading as calculated at the

Table 4.3. Bulk stress, resilient modulus, low-strain modulus and normalized resilient modulus for FWD, LSME and bench-scale tests.

Test Method	Bulk Stress (kPa)	Resilient Modulus (MPa)	Low-strain Modulus (MPa)	Normalized Resilient Modulus
Recycled Asphalt Pavement				
FWD	112	195	3076	0.06
LSME (0.20 m)	169	276	3969	0.07
LSME (0.30 m)	117	335	3161	0.11
Bench-Scale – External	110 – 858	128 – 345	3,042 – 10,867	0.04*
Bench-Scale – Internal	110 – 858	435 – 2,071	3,042 – 10,867	0.15*
Recycled Concrete Aggregate				
FWD	137	265	977	0.27
LSME (0.20 m)	159	360	1,058	0.34
LSME (0.30 m)	116	398	893	0.45
Bench-Scale – External	113 – 857	141 – 403	882 – 2,582	0.15*
Bench-Scale – Internal	113 – 857	484 – 1,644	882 – 2,582	0.56*
Blended RCA/Class 5				
FWD	117	225	895	0.25
LSME (0.20 m)	166	248	1,047	0.24
LSME (0.30 m)	116	341	893	0.38
Bench-Scale – External	109 – 867	142 – 428	868 – 2,204	0.17*
Bench-Scale – Internal	113 – 867	492 – 1,857	881 – 2,204	0.64*
Class 5				
FWD	127	97	619	0.16
LSME (0.20 m)	170	215	698	0.31
LSME (0.30 m)	118	297	601	0.49
Bench-Scale – External	95 – 839	94 – 326	550 – 1,344	0.20*
Bench-Scale – Internal	95 – 839	309 – 1,291	550 – 1,344	0.71*

* - Average value

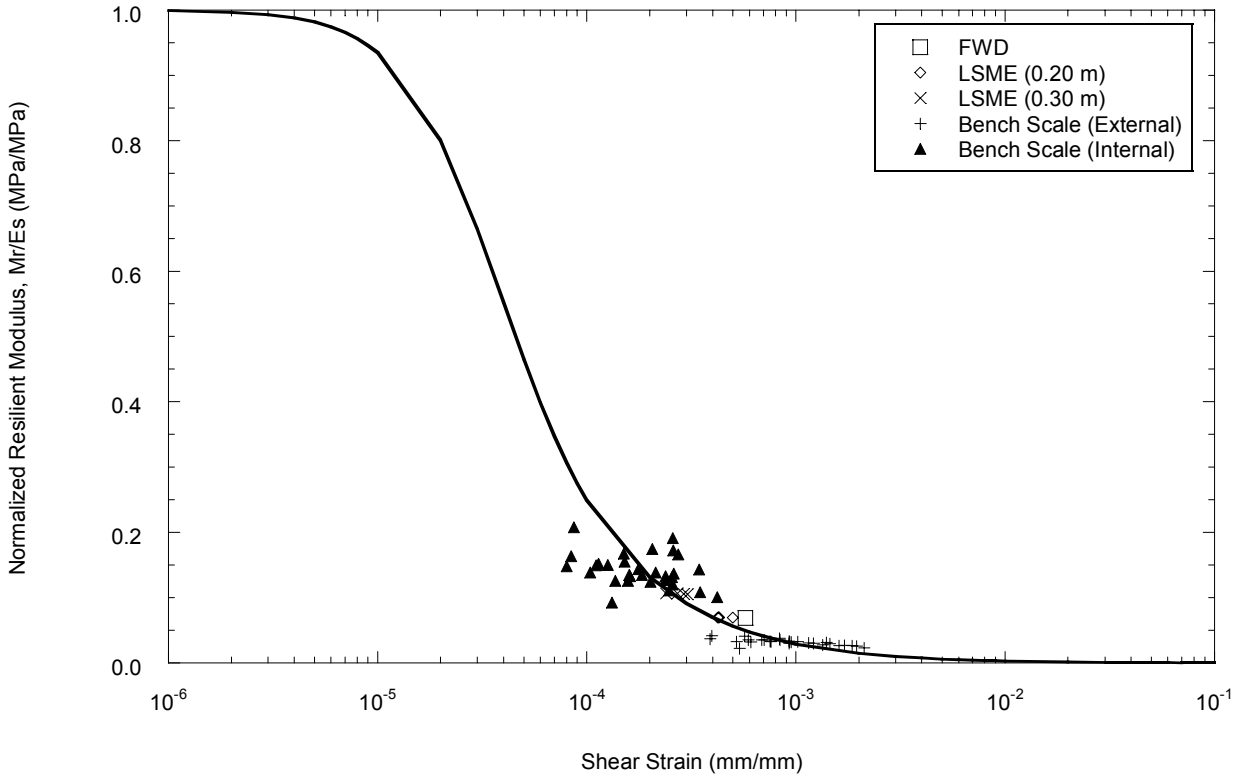

Fig. 4.25. Backbone curve fit to FWD, LSME and bench-scale data for RAP.

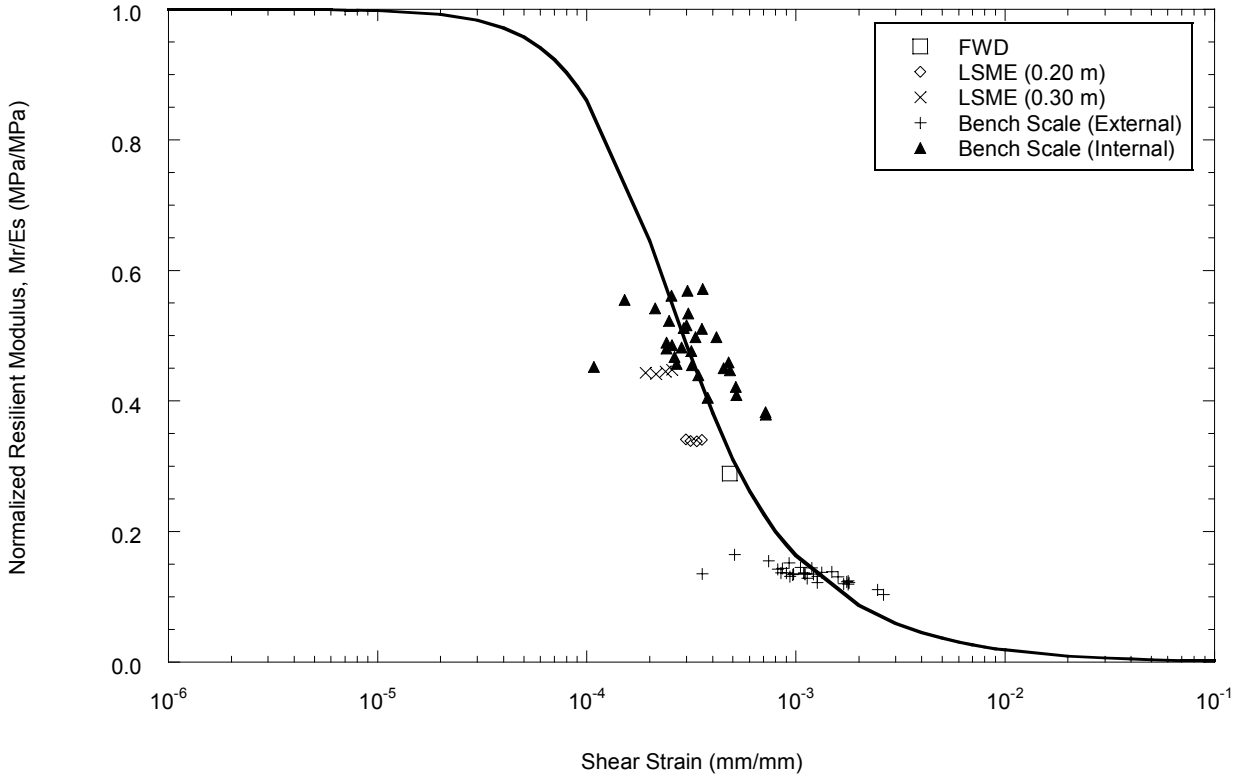

Fig. 4.26. Backbone curve fit to FWD, LSME and bench-scale data for RCA.

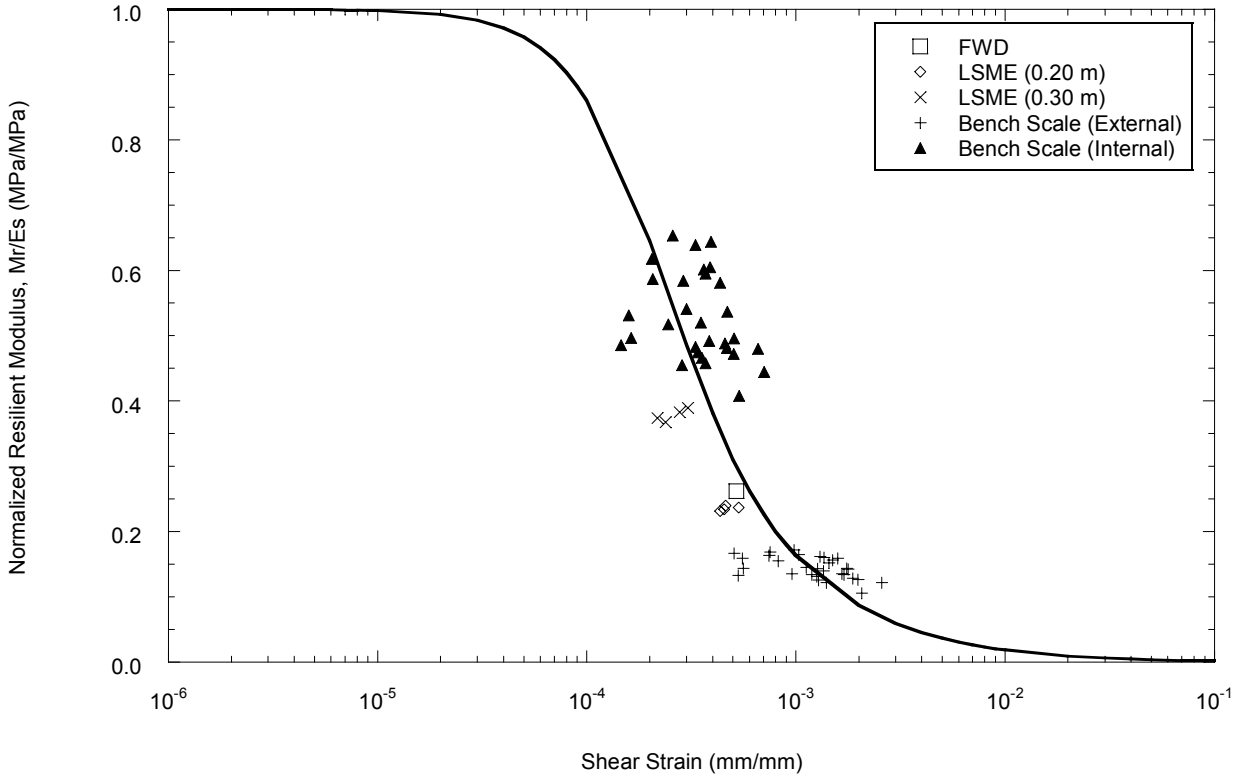

Fig. 4.27. Backbone curve fit to FWD, LSME and bench-scale data for blended RCA/Class5.

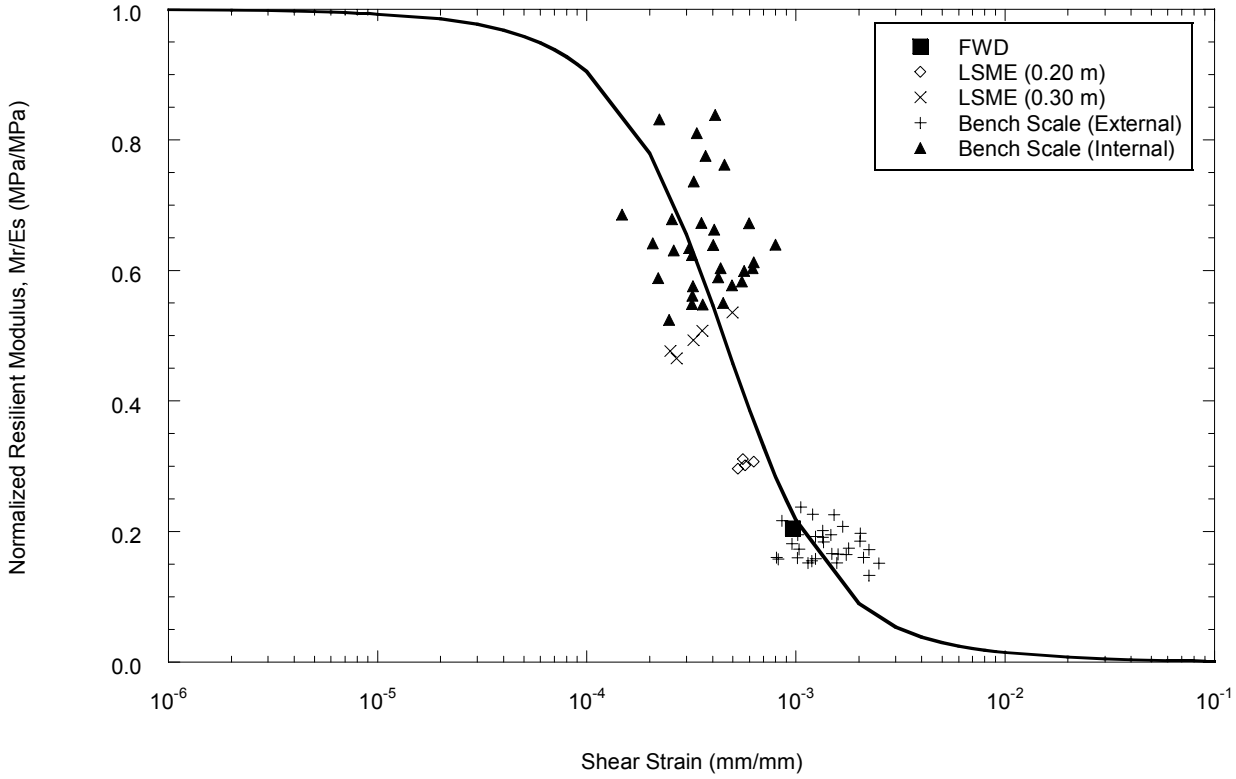

Fig. 4.28. Backbone curve fit to FWD, LSME and bench-scale data for Class 5.

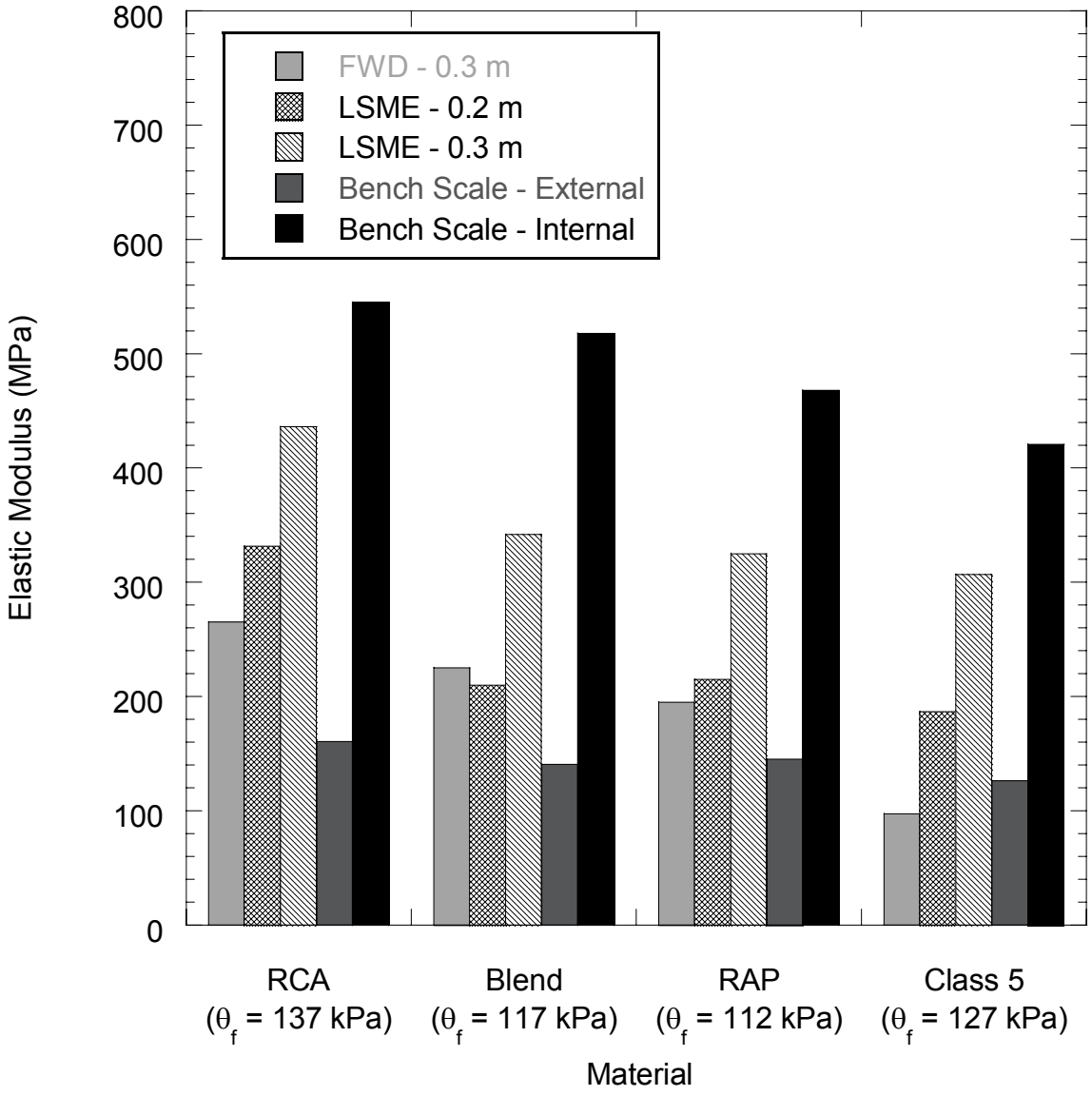

Fig. 4.29. Resilient modulus at field bulk stress (θ_f) for RAP, RCA, blended RCA/Class 5, and Class 5.

mid-depth of the layer using MICHPAVE. The resilient moduli of the LSME and bench-scale tests were recalculated for the field bulk stress using Eqn. 2.2. Table 4.3 summarizes the field bulk stress and resilient moduli determined for each loading test.

The low-strain modulus for each material at field bulk stress was calculated by multiplying the resilient modulus by the normalized resilient modulus. The low-strain resilient modulus at field bulk stress for each test method is presented in Fig. 4.30 and also summarized in Table 4.4. The variance of the low-strain (maximum) modulus determined for each test method is presented in Table 4.5. The coefficient of variance (c.o.v.) for RAP was the highest at 7.6%. The c.o.v. for RCA and blended material were approximately equal at 4.1% and 4.4%, respectively. The c.o.v. of the Class 5 was the smallest at 2.3%. For all materials, the coefficient of variance was 7.6% or less, indicating a reasonable amount of similarity between the test methods when properly scaled to the same bulk stress and strain level. It is also clear that different strain levels are induced in different tests resulting in varying resilient modulus depending on the test procedure even if at the same bulk stress. Bench-scale resilient modulus tests result in lower moduli based on externally measured deflections and in markedly higher moduli based on internally measured deflections in comparison to FWD or LSME moduli. LSME with 0.3-m thick layer (the same as in the field) resulted in higher moduli than the field moduli obtained from the FWD test. LSME moduli with 0.2-m thick layer were the closest to the field FWD moduli.

Table 4.4. Resilient modulus and low-strain modulus at field bulk stress.

Test Method	Resilient Modulus @ Field Bulk Stress (MPa)	Normalized Resilient Modulus	Low-strain Modulus (MPa)
Recycled Asphalt Pavement, Bulk Stress = 112 kPa			
FWD	195	0.06	3076
LSME (0.20 m)	215	0.07	3071
LSME (0.30 m)	325	0.11	2954
Bench-Scale – External	145	0.04	3625
Bench-Scale – Internal	468	0.15	3120
Recycled Concrete Aggregate, Bulk Stress = 137 kPa			
FWD	265	0.27	977
LSME (0.20 m)	332	0.34	976
LSME (0.30 m)	436	0.45	968
Bench-Scale – External	161	0.15	1073
Bench-Scale – Internal	545	0.56	973
Blended RCA/Class 5, Bulk Stress = 117 kPa			
FWD	225	0.25	895
LSME (0.20 m)	210	0.24	875
LSME (0.30 m)	342	0.38	900
Bench-Scale – External	141	0.17	829
Bench-Scale – Internal	518	0.64	809
Class 5, Bulk Stress = 127 kPa			
FWD	97	0.16	619
LSME (0.20 m)	187	0.31	603
LSME (0.30 m)	307	0.49	626
Bench-Scale – External	126	0.20	630
Bench-Scale – Internal	421	0.71	592

Table 4.5. Variance of low-strain elastic modulus obtained at field bulk stress.

Method	Low-strain Modulus at Field Bulk Stress (MPa)			
	RCA	RAP	Blend	Class 5
FWD	977	3076	895	619
LSME (0.20 m)	976	3071	875	603
LSME (0.30 m)	968	2954	900	626
Bench-Scale – External	1073	3625	829	630
Bench-Scale – Internal	973	3120	809	592
Mean Average	992	3160	863	614
Standard Deviation	40	239	38	14
Coefficient of Variance	4.1%	7.6%	4.4%	2.3%

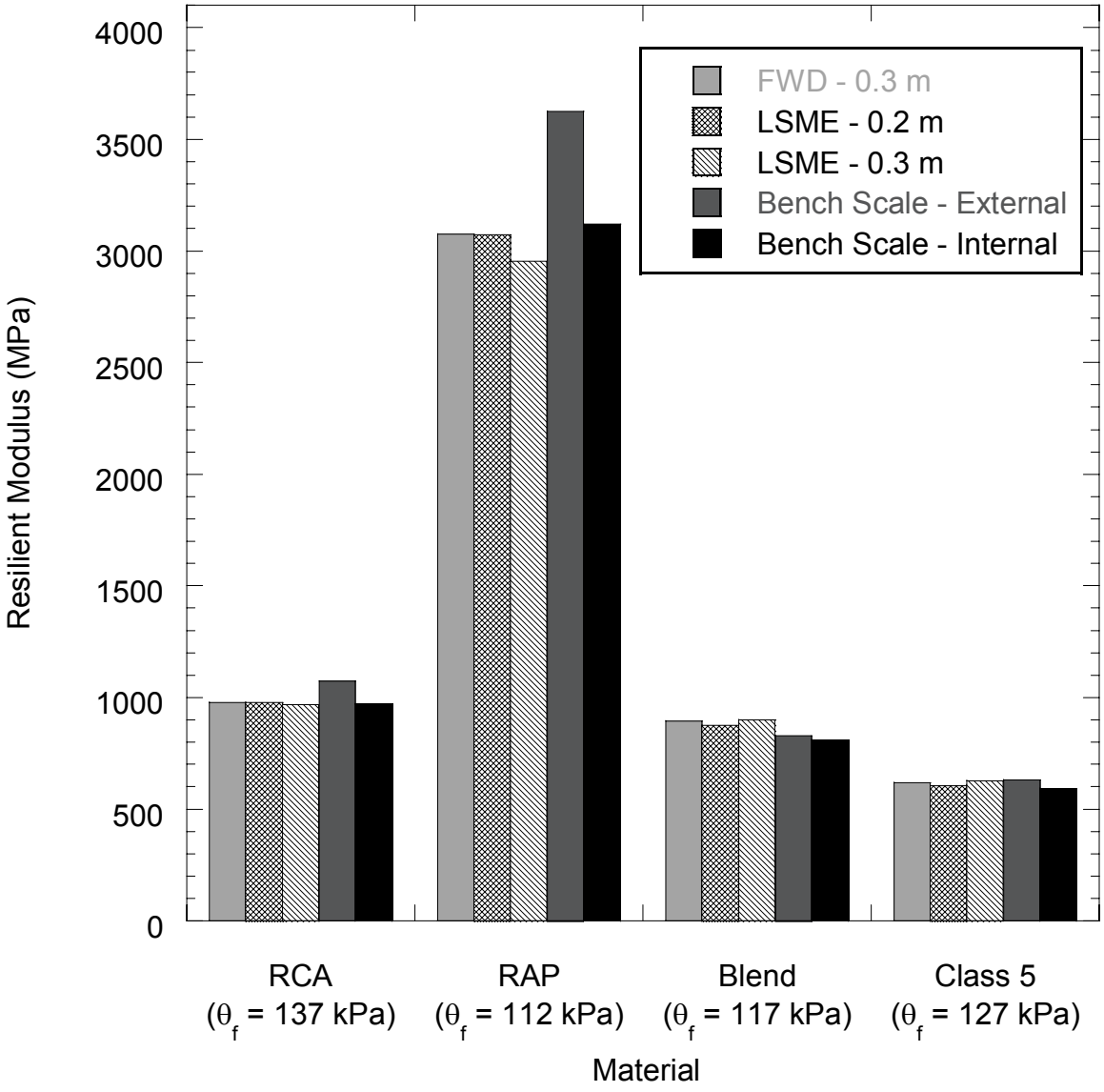

Fig. 4.30. Low-strain elastic modulus at field bulk stress (θ_f) for RAP, RCA, blended RCA/Class 5, and Class 5 as estimated from different test methods.

5. Summary and Conclusions

This laboratory investigation dealt with the determination of the resilient modulus of two recycled materials: recycled asphalt pavement (RAP) and recycled concrete aggregate (RCA). The investigation also dealt with the determination of the resilient modulus of one blended material consisting of approximately 50% RCA and 50% conventional base material (Class 5). The objectives were to assess the stiffness of recycled materials and to determine the scalability of laboratory results to field scale conditions. The objective was met by determining the resilient modulus of the recycled materials using large-scale model experiments (LSME) and comparing to the resilient modulus determined from bench-scale tests in accordance with NCHRP 1-28a and field scale tests using a falling weight deflectometer (FWD). The low-strain modulus of each material was also determined using seismic testing methods, and backbone curves (normalized modulus versus strain) were developed from the resulting stress-strain relationships. A conventional base course meeting the gradation standard of a Minnesota Department of Transportation Class 5 aggregate was used as a reference material in this study.

RAP experienced higher plastic deflections compared to the Class 5, while RCA experienced lower plastic deflections. The plastic deflection of RAP was approximately 211% and 402% greater than that of Class 5 for 0.2 m and 0.3 m layer thicknesses, respectively, and the plastic deformation of RCA was approximately 69% smaller than that of Class 5 for both layer thicknesses. Blended RCA/Class 5 experienced plastic deflections that were 39% and 20% smaller than Class 5 for layer thicknesses of 0.2 m and 0.3 m, respectively. For an increase in

layer thickness from 0.2 m to 0.3 m, base plastic deflections of RCA and Class 5 decreased 10% and 13%, respectively. Plastic deflection of RAP is 40% larger for 0.3-m layer thickness compared to 0.2-m layer thickness, which is attributed to the viscous nature of the asphalt coating the RAP particles. Plastic deformation of blended RCA/Class 5 is 13% larger for the same increase in layer thickness, which can most likely be attributed to experimental error. Conventional base course aggregate (Class 5) can be expected to contribute between 4 and 8% to an acceptable rutting depth of 13 mm. RCA and blended RCA/Class 5 can be expected to contribute 3 to 6% to the acceptable depth, and RAP can be expected to contribute 30 to 40%. Flexible pavements that incorporate RAP as a base course layer can be expected to encounter rutting problems. Flexible pavements that incorporate RCA and RCA/natural aggregate blends will experience rutting comparable to pavements that incorporate conventional base course aggregates.

The bench-scale resilient modulus tests with internally and externally measured deflections gave the highest and the lowest resilient moduli, respectively, the LSME tests with the 0.3 m and 0.2-m layer thicknesses having the second and third highest resilient moduli, respectively. The magnitudes of the tests are evenly spaced, and no direct correlation between the four methods can be discerned. The summary resilient modulus (SRM) of RCA was 42% to 77% higher than that of Class 5, whereas the SRM of RAP was 23% to 33% greater. The SRM of blended RCA/Class 5 was 18% greater than that of Class 5, which was comparable in magnitude to RAP. An increase in layer thickness from 0.2 m to 0.3 m had the effect of increasing the SRM of the materials from 130 MPa to 176 MPa. An increase in

RCA content increased the SRM at a rate that was non-linear, suggesting that the blended aggregate sample obtained in the field may have a composition other than the actual 50% RCA/50% Class 5.

Scaling was achieved by normalizing the resilient modulus of a material by the low-strain modulus and plotting the data as a function of the strain level at the corresponding stress state. The resulting plot for all four materials described a backbone curve which illustrates the stress-strain dependency of the given material. However, an uncharacteristically high low-strain modulus value for RAP greatly reduced the normalized resilient modulus and made the construction of a backbone curve difficult. This behavior is attributed to the bitumen coating the RAP particles causing the particles to adhere to each other, which leads to an increase in strain resistance at low stresses. Different test methods induce different strain levels at the same bulk stress, resulting in varying resilient modulus. Internally and externally measured bench-scale tests resulted in higher and lower resilient moduli, respectively, compared to FWD or LSME moduli. The LSME with 0.3 m-thick layer (the same as in the field) resulted in higher resilient modulus compared to the field moduli obtained from the FWD test. The LSME with 0.2-m thick layer resulted in resilient moduli which were close to the field FWD moduli. However, when properly scaled for the stress and strain levels, the low-strain modulus estimated from the different test methods are remarkably close to each other indicating the scalability of laboratory modulus to operating field modulus.

REFERENCES

ACPA (2009). "Recycling Concrete Pavements," *Bulletin B043P,* American Concrete Pavement Association, Skokie, IL.

Barksdale, R. D., and Itani, S. Y. (1989). "Influence of Aggregate Shape on Base Behavior," *Transportation Research Record*, No. 1227, Transportation Research Board, Washington, D.C., pp. 173–182.

Bejarano, M.O., Harvey, J. T., Lane, L. (2003). "In-Situ Recycling of Asphalt Concrete as Base Material in California", *Proc. 82nd Annual Meeting*, Transportation Research Board, Washington D.C. CD-Rom, 22 pp.

Bennert, T., Papp Jr, W. J., Maher, A. and Gucunski, N. (2000). "Utilization of Construction and Demolition Debris under Traffic-Type Loading in Base and Subbase Applications," *Transportation Research Record*, No. 1714, pp. 33-39.

Benson, C. H., Edil, T. B., Ebrahimi, A., Kootstra, R. B., Li, L., and Bloom, P. (2009). "Use of Fly Ash for Reconstruction of Bituminous Roads: Large-Scale Model Experiments," Minnesota Department of Transportation, St Paul, MN.

Blankenagel, B. J. and Guthrie, W. S. (2006). "Laboratory Characterization of Recycled Concrete for Use as Pavement Base Material," *Geomaterials*, No. 1952, pp. 21-27.

Brown, S. F., and Pell, P. S. (1967). ''An Experimental Investigation of the Stresses, Strains and Deflections in a Layered Pavement Structure Subjected to Dynamic Loads,'' *Proc, 2nd Int. Conf. Struct. Des. of Asphalt Pavements*, pp 487–504.

Burreglo, S. B., Yuan, D., Nazarian, S., (2009). "Cement Treated RAP Mixes for Roadway Base and Subbase: Evaluation of RAP Variability," *Technical Memorandum 0-6084-3*, Center for Transportation Infrastructure Systems, The University of Texas at El Paso, El Paso, TX.

Bush, A. J. and Alexander, D. R. (1985). "Pavement Evaluation Using Deflection Basin Measurements and Layered Theory," *Transportation Research Record* 1022, Transportation Research Board, National Research Council, Washington DC, pp. 16-29.

Camargo, F. F., Edil, T. B., Benson, C. H. (2009). “Strength and Stiffness of Recycled Base Materials Blended with Fly Ash,” *Proc. 88th Annual Meeting*, CD-ROM, 09-1971, National Research Council, Washington DC.

Chini, A. R., Kuo, S. S., Armaghani, J. M. and Duxbury, J. P. (2001). “Test of Recycled Concrete Aggregate in Accelerated Test Track,” *Journal of Transportation Engineering*, Vol. 127, No. 6, pp. 486-492.

Ebrahimi, A., Kootstra, B. R. , Edil, T. B., and Benson, C. H. (2010). "Equivalency-Based Design and Mechanical Properties of Recycled Roadway Materials With or Without Fly Ash Stabilization", *Proc. 89th Annual Meeting*, Transportation Research Board, Washington D.C, submitted.

Edil, T.B. and Fratta, D. (2009). "Development of Testing Methods to Determine Interaction of Geogrid-Reinforced Granular Material for Mechanistic Pavement Analysis," *Wisconsin Highway Research Program #0092-07-05*, Wisconsin Department of Transportation, Madison, Wisconsin.

Edil, T. B. and Luh, G. F. (1978). “Dynamic Modulus and Damping Relationships for Sands,” *Proc. Geotechnical Engineering Specialty Conference on Earthquake Engineering and Soil Dynamics*, American Society of Civil Engineers, Pasadena, California, Vol. I, pp. 394-409.

FHWA (2008). “User Guidelines for Byproducts and Secondary Use Materials in Pavement Construction,” *FHWA Report FHWA-RD-97-148*, Federal Highway Administration, McLean, Virginia.

Grogan, T. (1996). "Aggregate: Demand on a Roll," *ENR*, 237 (14), p 82.

Guthrie, W. S., Cooley, D. and Eggett, D. L. (2007). “Effects of Reclaimed Asphalt Pavement on Mechanical Properties of Base Materials,” *Transportation Research Record*, No. 2006, pp. 44-52.

Hardin, B.O. and Drnevich, V.P. (1972). “Shear Modulus and Damping in Soils: Design Equations and Curves,” *Journal of the Soil Mechanics and Foundation Division, Proceedings of the ASCE*, Vol. 98, No. SM7, pp. 667 – 692.

Harichandran, R. S., Baladi, G. Y., Yeh, M. (1989). “Development of a Computer Program for Design of Pavement Systems Consisting of Bound and Unbound Materials,” Dept. of Civil and Environmental Engineering, Michigan State University, Lansing, Michigan, 1989.

Hicks, R. G. (1970). “Factors Influencing the Resilient Properties of Granular Materials,” PhD Thesis, University of California, Berkeley, Berkeley, CA.

Hicks, R. G., and Monismith, C. L. (1971). ‘‘Factors Influencing the Resilient Properties of Granular Materials,’’ *Highway Research Record 345*, pp 15–31.

Huang, Y. (2004). *Pavement Analysis and Design*, 2nd Ed., Prentice-Hall, Inc., Upper Saddle River, New Jersey.

Johnson, A., Clyne, T. R., and Worel, B. J. (2009). "2008 MnROAD Phase II Construction Report," Minnesota Department of Transportation, Maplewood, Minnesota.

Kim, W., Labuz, J. F. and Dai, S. (2007). “Resilient Modulus of Base Course Containing Recycled Asphalt Pavement,” *Transportation Research Record*, No. 2006, Transportation Research Board, National Research Council, Washington, DC, pp. 27-35.

Kim, D. S., and Stokoe II, K. H. (1992). “Characterization of Resilient Modulus of Compacted Subgrade Soils Using Resonant Column and Torsional Shear Tests,” *Transportation Research Record*, No. 1369, Transportation Research Board, National Research Council, Washington, DC, pp. 83-91.

Kolisoja, P. (1997). “Resilient Deformation Characteristics of Granular Materials,” PhD Thesis, Tampere University of Technology, Pub. No. 223, Tampere, Finland.

Kootstra, B. R., Ebrahimi, A., Edil, T. B., and Benson, C.H. (2010). "Plastic Deformation of Recycled Base Materials,” *GeoFlorida’2010*, ASCE Geo Institute, submitted.

Kramer, S.L. (1996). *Geotechnical Earthquake Engineering*. Prentice Hall. Upper Saddle River, NJ.

Kuo S. S., Mahgoub, H. S. and Nazef, A. (2002). “Investigation of Recycled Concrete Made with Limestone Aggregate for a Base Course in Flexible Pavement”, *Geomaterials*, No. 1787, pp. 99-108.

Lekarp, F., Isacsson, U., and Dawson, A. (2000). ‘‘State of the Art. I: Resilient Response of Unbound Aggregates,” *Journal of Transportation Engineering*, ASCE, 126(1), pp 66–75.

Li, L., Benson, C. H., Edil, T. B., Hatipoglu, B., and Tastan, E. (2007). “Evaluation of Recycled Asphalt Pavement Material Stabilized with Fly Ash,” *ASCE Geotechnical Special Publication* (CD-ROM), 169 pp.

Molenaar, A. A. A. and Van Niekerk, A. A. (2002). “Effects of Gradation, Composition, and Degree of Compaction on the Mechanical Characteristics of

Recycled Unbound Materials," *Transportation Research Record: Journal of the Transportation Research Board*, Transportation Research Board, Washington, D.C., No. 1787, pp. 73-82.

Monismith, C. L., Seed, H. B., Mitry, F. G., and Chan, C. K. (1967). "Prediction of Pavement Deflections from Laboratory Tests," *Proc. 2nd Int. Conf.. Struct. Des. of Asphalt Pavements*, pp 109–140.

Morgan, J. R. (1966). "The Response of Granular Materials to Repeated Loading," *Proc. 3rd Conf.,* ARRB, pp 1178–1192.

Nataatmadja, A. (1992). ''Resilient Modulus of Granular Materials Under Repeated Loading,'' *Proc., 7th Int. Conf. on Asphalt Pavements*, Univ. of Nottingham, Nottingham, U.K., 1, pp 172–185.

Nataatmadja, A. and Tan, Y. L. (2001). "Resilient Response of Concrete Road Aggregates," *Journal of Transportation Engineering*, Vol. 127, No. 5, pp 450-453.

Plaistow, L. C. (1994). "Non-Linear Behavior of Some Pavement Un-bound Aggregates," MS Thesis, Dept. of Civil Engineering, University of Nottingham, Nottingham, England.

Poon, C. S., Qiao, X. C. and Chan, D. X. (2006). "The Cause and Influence of Self-Cementing Properties of Fine Recycled Concrete Aggregates on the Properties of Unbound Sub-Base," *Waste Management*, Vol. 26, No. 10, pp. 1166-1172.

Richart, F.E., Jr., Hall, J.R., and Woods, R.D. (1970). *Vibrations of Soils and Foundations*, Prentice Hall, Inc., Eaglewood Cliffs, NJ.

Santamarina, J.C., Klein, K.A., and Fam, M.A. (2001). *Soils and Waves*. John Wiley & Sons Ltd., West Sussex, England, 488 pp.

Schuettpelz, C. (2008). "Evaluation of the Influence of Geogrid Reinforcement on Stiffness in Compacted Base Course Material," MS Thesis, University of Wisconsin-Madison, Madison, WI.

Seed, H. B., Mitry, F. G., Monismith, C. L., and Chan, C. K. (1967). ''Prediction of Flexible Pavement Deflections from Laboratory Repeated Load Tests.'' *NCHRP Rep. No. 35*, National Cooperative Highway Research Program.

Seed, H. B. and Idriss, I. M. (1970). "Soil Moduli and Damping Factors for Dynamic Response Analyses," *Report No. EERC 70-10*, University of California, Earthquake Engineering Research Center, Berkeley, CA, 1970.

Son, Y. H., (2010). "Resilient Moduli of Recycled Materials," Personal Communication.

Tanyu, B.F., Kim, W. H., Edil, T. B., and Benson, C. H., (2003). "Comparison of Laboratory Resilient Modulus with Back-Calculated Elastic Moduli from Large-Scale Model Experiments and FWD Tests on Granular Materials," *Resilient Modulus Testing for Pavement Components*, ASTM STP 1437, G. N. Durham, W. A. Marr, and W.L. De Groff, Eds., ASTM International, West Conshohocken, Pa.

Thom, N. H., and Brown, S. F. (1988). "The Effect of Grading and Density on the Mechanical Properties of a Crushed Dolomitic Limestone,'' *Proc. 14th ARRB Conf.*, Vol.14, Part 7, pp 94–100.

Thom, N. H., and Brown, S. F. (1989). ''The Mechanical Properties of Unbound Aggregates from Various Sources,'' *Unbound Aggregates in Roads*, R. H. Jones and A. R. Dawson, eds., pp 130–142.

Van Niekerk, A. A., Houben, L. J. M., and Molenaar, A. A. A. (1998). "Estimation of Mechanical Behavior of Unbound Road Building Materials from Physical Material Properties," *Proc., 5th Int. Conf. on the Bearing Capacity of Roads and Airfields*, R. S. Nordal and G. Rafsdal, eds., Vol.3, pp 1221–1233.

Wen, H. and Edil, T. B. (2009). "Sustainable Reconstruction of Highways with In-situ Reclamation of Materials Stabilized for Heavier Loads," *Proc. 2nd Int. Conf. on Bearing Capacity of Roadway, Railways and Airfields*, Urbana-Champaign, IL, CD-ROM.

WisDOT (2009). "Layer Coefficient Values for Cracked and Seated Concrete," *Transportation Synthesis Report,* Wisconsin Department of Transportation, Madison, Wisconsin.

APPENDIX A

IMPLEMENTATION OF ABBREVIATED TEST PIT AREA

A.1 Introduction

Previous testing using the LSME incorporated the entire 3.0 m x 3.0 m test area to measure deflections and determine the resilient modulus for a given base course material under cyclical loading. However, limited amounts of base course material available for testing made it necessary to reduce the evaluated test area within the LSME to 1.0 m x 1.0 m. The remainder of the 3.0 m x 3.0 m test area was made up of recycled pavement material (RPM) to maintain the boundary stress that would otherwise be lost by a reduction in test area. The equivalency of the abbreviated LSME test area to the full LSME test area was determined by comparing the resilient modulus of RPM obtained using both test methods.

The RPM was compacted to a thickness of 0.3 m within the entire 3.0 m x 3.0 m LSME test area according to methods described in section 3.3.1. The abbreviated 1.0 m x 1.0 m test area was then excavated in the center of the LSME test area, leaving approximately 2.0 m of RPM around the LSME perimeter, as shown in Fig. A.1. The exposed subgrade was loosened and recompacted prior to placement of the specimen material to establish a consistent initial density that would be repeated for all subsequent tests. The circumference of the abbreviated test area was lined with nonwoven, heat bonded geotextile to separate the RPM from the test specimen and allow confinement of the test specimen from the surrounding RPM, as shown in Fig.A.2. RPM was recompacted within the abbreviated test area and the summary resilient modulus of the tested material was determined using methods described in section 3.3.4.

Fig. A.1. Overview of abbreviated test pit area prior to material placement.

Fig. A. 2. Placement of RPM within abbreviated test pit area.

The resilient modulus of the RPM determined for the abbreviated test area was measured to be 538 MPa. Benson et al. (2009) reported a summary resilient modulus of 505 MPa on LSME tests for the same material using the full 3.0 m x 3.0 m test area. Using the smaller test area increased the summary resilient modulus by approximately 6%. A comparison of the summary resilient modulus determined for the two specimen sizes is presented in Fig. A.3. The summary resilient moduli determined for the 0.3-m thick LSME tests on RAP, RCA, blended RCA/Class 5 and Class 5 as discussed in section 4.2 are also presented in Fig. A.3. for scale. The magnitude of the RPM resilient modulus is similar for both the full and abbreviated test pit areas. Boudreau (2003) tested the repeatability of bench-scale resilient modulus tests and found that the coefficient of variance was as high as 4.5% for specimens tested at the same stress level. The mean average and the standard deviation measured between the two tests were 522 MPa and 23 MPa respectively, indicating a coefficient of variance of 4.4%. Assuming a correlation between the bench-scale and LSME tests, the two test methods are within an acceptable amount of variance.

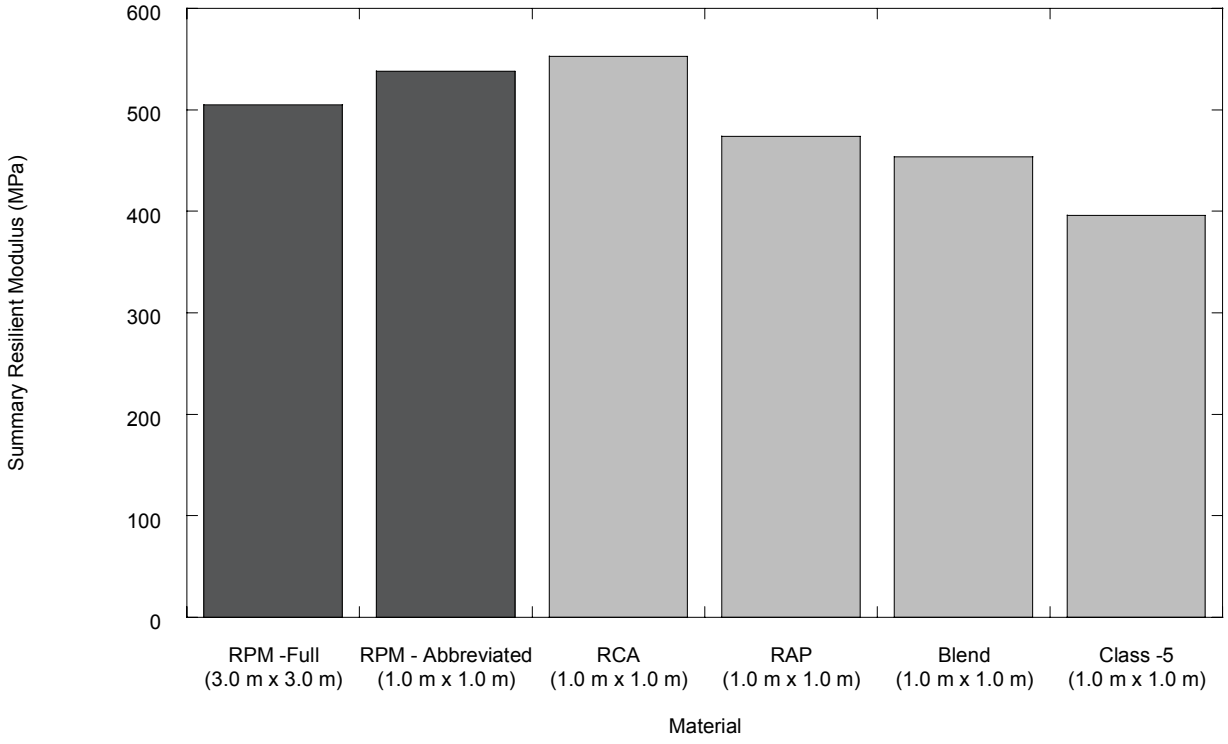

Fig. A.3. Comparison of resilient modulus of RPM obtained for full and abbreviated test pit areas with RCA, RAP, blended RCA/Class 5 and Class 5 obtained for abbreviated test pit area.

APPENDIX B

DETERMINATION OF LAYER COEFFICIENTS

B.1 Determination of Layer Coefficients

The design of pavement structures is dependent on the determination of appropriate layer thicknesses based on the mechanical properties of the associated pavement layers. The AASHTO design procedure relates the structural capacity of a given layer to a structural number, SN_i, which is defined as the product of the layer thickness, D_i, and layer coefficient, a_i. The SN for the pavement structure as a whole is calculated according to Eqn. B.1.

$$SN = SN_1 + SN_2 m_2 + SN_3 m_3 = a_1 D_1 + a_2 D_2 m_2 + a_3 D_3 m_3 \quad \text{(B.1)}$$

The variable m_i is the drainage modification facto, which is assumed to be 1.0 for the base materials used in this study. Design layer thicknesses are chosen in such a way that the resulting SN is greater than or equal to a required SN. The required SN is typically determined based on estimated traffic, serviceability loss, and effective roadbed resilient modulus (AASHTO 1993).

The layer coefficient measures the relative ability of a unit thickness of a given material to function as structural component in a pavement (Haung 2007). The layer coefficient for untreated base course can be estimated from the resilient modulus of the layer according to the relationship proposed by Rada and Witczak (1981) and presented in Eqn. B.2.

$$a_2 = 0.249(\log M_r) - 0.977 \quad \text{(B.2)}$$

where M_r is the resilient modulus measured in psi.

The layer coefficients were calculated for the 0.2-m and 0.3-m thick layers tested in the LSME using the SRM according to Eqn. B.2 for RAP, RCA, blended RCA/Class 5 and Class 5. The relationship between layer coefficient and layer

thickness for these materials is presented in Fig. B.1. The SN for each of the base course materials tested in the LSME was calculated as the product of the layer thickness (in inches) and the associated layer coefficient. The SN and layer coefficients for each LSME test are presented in Table B.1.

The magnitude of the layer coefficients follow the hierarchy seen previously for SRM, with RCA and Class 5 having the highest and lowest values, respectively, and RAP and blended RCA/Class 5 having the second and third highest values, respectively. The layer coefficients of RAP, blended RCA/Class 5, and Class 5 all increased at the same rate with an increase in layer thickness. The layer coefficient of RCA increased with increased layer thickness as well, albeit at a much slower rate. The Class 5 layer coefficients of 0.16 and 0.21 determined for the LSME layer thicknesses of 0.2 m and 0.3 m, respectively, are marginally higher than typical values for granular base course of 0.10 and 0.14 (Huang 2004). RCA had layer coefficients of 0.21 and 0.24 for layer thicknesses of 0.2 m and 0.3 m, which is within typical values for rubblized concrete as reported by WisDOT (2009).

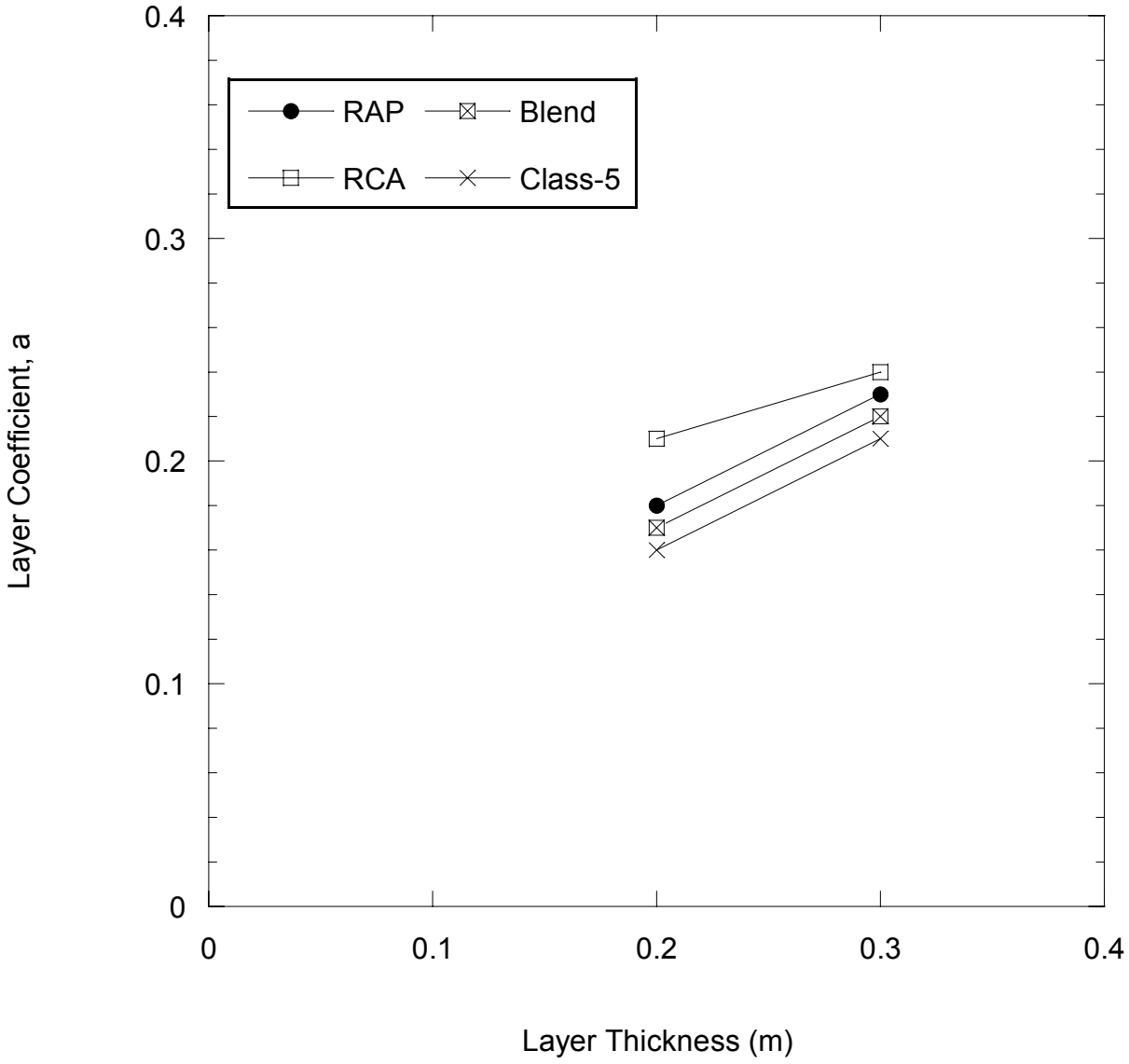

Fig. B.1. Layer coefficient vs. base layer thickness for RAP, RCA, blended RCA/Class 5, and Class 5.

Table B. 1. Layer coefficients and structural numbers for different LSME thicknesses.

Material	Layer thickness (m)	Summary Resilient Modulus (kPa)	Layer Coefficient, a_2	Structural Number, SN
RAP	0.2	314	0.18	1.44
	0.3	474	0.23	2.76
RCA	0.2	418	0.21	1.68
	0.3	553	0.24	2.88
Blended RCA/Class 5	0.2	278	0.17	1.36
	0.3	454	0.22	2.64
Class 5	0.2	243	0.15	1.2
	0.3	396	0.21	2.52